

# “Circulation of the Turkish Straits System under interannual atmospheric forcing”

Aydoğdu et al., 2018, in revision, submitted to Ocean Science

## General response to all the reviewers

We are grateful to the anonymous referees for their careful assessment and Dr. Zhang and Dr. Ferrarin for their short comments on the original manuscript of our study on the circulation of the Turkish Straits System. Their comments and suggestions have helped us to substantially improve the manuscript. Below are our point-by-point responses to their comments, which should resolve all points raised by the referees towards publication of our work. Our proposed modifications in line with the present responses are enclosed at the end of this document in a marked-up version of the manuscript, where the figure and table numbering used in the following responses are referenced to the marked-up version. The reviewers' comments and our responses are in italic and normal fonts, respectively, throughout this document, whereas the captions are given in bold fonts.

### Author' response to RC#1

*The manuscript is a generally well-written study about the Turkish Strait system. The manuscript has potential, because it completes some other studies and provides an overview on the general circulation in the Marmara Sea. However, it has some shortcomings that have to be addressed before the manuscript can be published.*

#### **General comments**

*How is the wind stress and pressure gradient in the BS dealt with? If you do not have the whole basin, the influence of these forces might not be represented well in the area that is part of your domain.*

We impose wind stress over the entire model area, following the earlier development in the Mediterranean Sea making use of a closed Atlantic box similar to ours (Tonani et al., 2008), which only has been configured to allow to understand the main wind-driven circulation characteristics. We do not apply atmospheric pressure forcing, because that would require having proper set of open lateral boundary conditions in the Aegean and Black Sea boxes with a potential to excite basin-modes in the adjacent basins that we initially try to exclude from our simulations.

*The boundary conditions are prescribed in a strange way. Authors claim to use a buffer zone to relax salinity, but then they use a time scale of 2 days. This is, for a large basin like this, basically equal to imposing the salinity.*

We indeed impose a monthly climatology for salinity in the buffer zone with a short relaxation time because we want to fix strictly the salinity value in the buffer zone to adequately represent major freshwater effects that should feed back to the TSS region where our main interest is concentrated.

*Validation is not strict. Authors show that they get the orders of magnitude right. But this is not a real validation.*

The observational data at the scale of the Marmara Sea is scarce and to our knowledge we have made use of all the data available for a basin-scale validation of the T, S properties. In addition, we have compared the Bosphorus Strait with the available current data of Jarosz et al. (2011, 2012) during the experiment period. Table 2 shows the quantitative estimates of the RMSE for temperature and salinity. Moreover, the sea level in the Marmara Sea is quantitatively compared with a four-year time series of observations obtained from tide gauges.

*Authors talk a lot about wind forcing, but it is not clear if pressure gradients are also accounted for.*

We do not consider atmospheric pressure, since we limit our attention to wind-driven part of the circulation as already stated. We now have explicitly commented this in Appendix A, where the model equations are presented. We also changed our title to read as:

“Circulation of the Turkish Straits System under interannual atmospheric forcing”

*Authors also use a correction term in order to conserve mass and salinity. However, as I have understood, they applied this correction term at every time step. This means they do not allow for variations in mass and salinity in the basin. However, I guess that the Danube discharge will lead to a variation of these parameters. So, these variations are completely suppressed. I think the authors will have to come up with another scheme that allows for variations and corrections are imposed in the long run.*

The total volume of the model needs to be conserved since the basin is closed, while also to counter resultant climate drift. We prefer to keep the volume to remain unchanged at every time step because that is the simplest choice in the absence of *a priori* information on how secular variations of the various flux components are balanced on climatological time scales. In order to have the basin averaged sea level tendency to vanish, we need to correct the surface boundary conditions for the vertical velocity to have zero mean vertical velocity.

Because of the dominating influence of the fresh-water term R in the Black Sea, the average of the net water flux (E-P-R) is not zero. We therefore needed to correct the vertical velocity, as applied by Tonani et al. (2008) for regional domains or by Gent et al. (1998) for the global ocean.

The reasoning is the same for salinity. We conserve the total salinity strictly, however, this does not prevent spatial variation of salinity since the correction is applied to the surface layer equally.

*The biggest problem for me is with table 4. If I check the difference between ingoing and outgoing fluxes at the Bosphorus, I get a volume difference that corresponds to about 8 meter of water level per year. This clearly cannot be. Authors should check their data and carefully check the volume balance.*

We gratefully acknowledge the reviewer’s close attention to volume transport calculated by the model. In addition, extensive discussion is now provided in relation to the volume transport issues brought to

our attention by the above comments and also by comment #3 of reviewer #2. The calculation of fluxes was indeed not very accurate and now they are corrected in Table 4 as well as in Fig. 14.

The major problem in the computation of volume transport was that we used daily snapshot velocities instead of daily mean velocities. We also had some inaccuracies in the post-processing computations of transport on the unstructured grid. Both sources of inaccuracy have now been eliminated to yield correct transport estimates. The net transport difference between the northern and southern sections of the Bosphorus Strait is now computed as  $0.5 \text{ km}^3/\text{yr}$ , with the higher value in the northern section.

On the other hand, the reduction of transport as one moves from north to south along the TSS is a direct result of our present correction scheme necessitated by volume conservation in the model domain with closed lateral boundaries. As applied here, the correction scheme results in a continuous decrease of transport along the way from the Black Sea to the Aegean Sea by extracting water from the surface to balance the runoff water flux  $R$  introduced at the buffer zone minus the specified surface flux  $E-P$  up to the same point as discussed in Appendices A and B. We further discuss the effects of surface flux corrections on the Marmara Sea in our response to reviewer #2. We refer to sections 3.1 and 3.3 in the marked-up version of the manuscript respectively for the surface water fluxes and the resulting volume transports.

### **Specific comments**

*1,3 interface where?*

We remove the phrase 'interface layer' and use 'pycnocline'. The sentence now reads as: “The depth of the pycnocline between the upper and lower layers remains stationary after six years of integration...”

*3,22 differ from what*

The sentence is clarified as “... differ significantly in each of their experiments with ...”

*Fig 1 does this show the whole model domain?*

This is the whole model domain. We clarify it in the caption.

*5,14-16 how is the salinity of BS and Med kept on a constant level?*

The salinity in the model domain evolves throughout the simulation according to water and heat fluxes from the atmosphere and the river runoff flux supplied through the Black Sea buffer zone. Therefore, it varies spatially in the model domain. The salinity in the Black and Mediterranean Seas are not kept constant but the volume salinity is conserved over the whole model domain by the correction term in Appendix B.

*5,24 is evaporation considered?*

Yes, and it is shown in Fig. 3 for the Marmara Sea. We now have added a similar figure for the whole

domain with units for the water fluxes converted to  $\text{km}^3/\text{yr}$  in order to extend our discussion on volume fluxes in the Marmara Sea and the Straits. Related section 3.1 is modified accordingly.

*Table 1 please define R and S*

We have included the notation R after “river discharges” and S\* after “salinity relaxation” in parenthesis in the caption.

*7,3 runoff is imposed, right? Salinity is relaxed in the buffer zone? Why not prescribe it on the boundary? A relaxation time of two days is practically equal to imposing this value. By the way, what about the other closed boundary, the Mediterranean? How has this boundary been handled?*

In order to prescribe an “entering volume flux” in the fully closed model basin and properly account for mass conservation, we imposed the vertical velocity boundary condition (A9). The Black Sea river runoff is distributed at the surface in the Black Sea buffer zone at the furthest limit of the model area excluding the actual major rivers. Moreover, we tightly relaxed salinity to monthly climatology values in the same box to keep realistic values of salinity entering in the Bosphorus.

In the simulation presented in the paper, we only have a buffer zone in the Black Sea. However, earlier tests using an additional buffer zone near the Aegean southern boundary were presented by Gürses et al. (2016), producing comparable results.

*Fig 3 the units for water fluxes need clarification. They are probably  $\text{m}^3/\text{s}$  per  $\text{m}^2$ , but this might not be obvious for the reader (it was not for me).*

We now present the water fluxes in  $\text{km}^3/\text{yr}$  in Fig. 3 to be comparable with the units of the volume transport through the straits.

*8,1  $Q_H$  is positive when? From atmosphere to ocean?*

Correct. We add it to the corresponding sentence as “... $Q_H$  is the heat flux (positive towards the ocean)...”

*11,4-7 I would like to point out the problem with T after 6 years of integration in deeper layers. As can be seen from figure 9 the lower layers have warmed up by nearly 2 degrees. What is the explanation for this behavior?*

If we understood correctly, the reviewer points out the difference between the observed and simulated temperature in the lower layer. We know that the lower layer water masses take several years to evolve after initialization, as can be seen in the trend in Fig.7. On the other hand, we also note that the observations in June 2013 are  $1^\circ\text{C}$  cooler than the ones in April and October 2008 although the 2013 summer measurements normally are expected to be warmer, possibly indicating such interannual changes in the sub-halocline water. The physical reason behind the observed variability could be the strong cooling event in 2012 (e.g. Benetazzo et al. 2014), which is not reproduced by the model; a side-effect that should be further investigated in the future.

*Fig 11 when you discuss wind forcing, you should also discuss atmospheric pressure forcing. What about pressure gradients over the same period? I guess pressure is included in the model equations, right?*

We do not investigate the short-term atmospheric pressure effects investigated because we only study the TSS circulation developed under the effects of the surface and lateral fluxes of water, heat and salt in this paper.

*13,1-2 wind forcing is not the only responsible for sea level fluctuations. Did you look in the pressure variations?*

Again, we do not have the atmospheric pressure included at the moment.

*13,7 why excluding pressure forcing?*

In the present study, we are mainly interested in the circulation developed in the TSS region, i.e. the two Straits and the Marmara Sea, focusing on the impacts of the wind forcing as well as water and heat fluxes on a regional scale. The main reasons to exclude the pressure forcing were to limit unintended feedback of motions that could independently develop in the falsified (cut-down) geometries of the Aegean and Black Sea boxes, including unrealistic basin modes that could be excited by the large scale atmospheric pressure field in these closed basin reservoirs. We believe that to adequately represent atmospheric pressure effects on a small dimension regional model, one needs to have open boundary conditions applied on a realistic domain.

*Table 4 The net flow should be really exactly the same for the northern and southern location. If I assume the length of the Bosphorus with 30 km and its average width with 3 km, I get an area of 100 km\*\*2. The net flux difference between northern and southern sections is 0.8 km\*\*3. This would correspond to an 8 m water level difference over one year. This clearly cannot be true. So what is wrong with this calculation? The way you compute fluxes, or your numbers? Please clarify.*

We responded to this question of the reviewer in the general comments. The issue related to volume transports is discussed extensively also in response to the comment #3 of the reviewer #2.

*17,5 also normalized by the density*

We added “normalized by density” in the figure caption and text.

*17,10 eq. 3 has no right hand side. . .*

Thanks. We rephrase the sentence as “...we normalize the integral in (3) by the volume...”

*18,1 is this total kinetic energy, or only the one caused by wind effects?*

This is total kinetic energy. We remove the word “resulting” to avoid confusion.

*19,8 ?????*

It is a latex related typo. Question marks are removed.

**Appendix:**

*A1 diffusion term. Sure about the 4th derivative in the term with  $A_h$ ? Ok, you use bi-harmonic diffusion.*

Correct.

*24,2 what about unstable stratification? Can you resolve problems arising with this small vertical diffusivity?*

The “background” vertical viscosity and diffusivity are minimum thresholds. Typically, the spatially varying vertical viscosity and the diffusivity are approximately two orders of magnitude greater than the background values. Therefore, there is no stability issue arising due to small vertical diffusivity.

*24,13 what does it mean, normalized to the buffer zone?*

That simply means that the water volume flux is divided by the buffer zone area to distribute it equally in the buffer zone in units of vertical velocity. We have rephrased the sentence.

*26,10 I do not understand: you compute the correction term at every time step? So you do not allow the model to become more or less saline during special events (spring river run off, etc.)? I would have done this computation on a mean (maybe annual) value. You clearly do not want a drift of salinity, but variations should be allowed*

We compute the correction terms  $W_{corr}$  and  $S_{corr}$  at every time step because we insist to conserve the mass and the volume at all times in the closed basin configuration. This requirement could in fact be released in the future if a priori information on all the water flux components, e.g. if the riverine, Bosphorus and surface components and their T, S characteristics had existed or alternatively, open boundary conditions could be accurately specified. In the present case of closed basin configuration, we prefer to abide by the requirements of mass conservation. This doesn't hinder daily or seasonal variation in the TSS region, which is the area of our main interest. The seasonal cycle in the Marmara Sea can be clearly seen in Fig. 7 even for the volume mean salinity.

**References**

Benetazzo, A., A. Bergamasco, D. Bonaldo, F. Falcieri, M. Sclavo, L. Langone, and S. Carniel(2014). Response of the adriatic sea to an intense cold air outbreak: Dense water dynamics and wave-induced transport. *Progress in Oceanography* 128, 115 – 138.

Gent, P. R., Bryan, F. O., Danabasoglu, G., Doney, S. C., Holland, W. R., Large, W. G., & McWilliams, J. C. (1998). The NCAR climate system model global ocean component. *Journal of Climate*,11(6), 1287-1306.

Tonani, M., Pinardi, N., Dobricic, S., Pujol, I., & Fratianni, C. (2008). A high-resolution free-surface model of

the Mediterranean Sea. *Ocean Science*, 4(1), 1-14.

## Author' response to RC#2

Authors use one model with a very good record (FESOM) and apply it to a unique ocean region, the Marmara Sea. I find the dynamics of Marmara Sea a novel topic. It is oceanographically interesting because circulation in the Marmara Sea is strongly dependent on the exchange with the neighboring basins, the Black Sea and the Mediterranean. However, I find some fundamental problems with this manuscript exactly in this part and do not recommend publishing it. With the following comments, I want to elucidate the basic problems, and help authors sharpen their paper if they want to submit a new manuscript.

### Major comments

#### *1. What is strongly needed is that authors*

*a) Demonstrate the power of using an unstructured-grid model compared to structured grid models when addressing the dynamics as dependent on the transport in the Straits of Bosphorus and Marmara. There are some references to earlier works, but there is not a critical comparison with structured grid models. Is the skill of unstructured-grid model and the proposed setup better in comparison to what is known from earlier works on the Marmara Sea modelling*

To our knowledge, the only structured grid model implementation in the whole Turkish Straits System (TSS) is the MITgcm configuration of Sannino et al. (2017) that used a curvilinear grid resolving the straits with higher resolution compared to the neighbouring basins. Other structured grid model implementations are used to simulate only individual components of the TSS, and not the full TSS as we intend to fully resolve fine geometries of fine scale flow features such as the two narrow straits in the present paper. On the other hand, there may be other ongoing attempts aiming to study inter-basin interactions by coarse structured grids facing immense computing requirements could not possibly resolve the complex, narrow straits and their adjacent regions to converge to realistic results. We have not attempted to review such cases as they would be outside our area of interest.

In Sannino et al. (2017), the focus is on the response of the TSS to a range of varying barotropic volume flux, whereas in our study, we focus on the impact of atmospheric forcing on the circulation in the Marmara Sea. Therefore, it is not possible to compare directly the two studies. However, we tried to identify some links between the simulated circulation in both studies in sections 3.3 and 3.4 as well as in the summary and discussion sections of the manuscript.

*b) Clearly demonstrate the superiority of FESOM compared to other unstructured grid models in the present study. Critical statements in the introduction about possible problems in other unstructured grid models need to be supported by a deeper analysis of results and inter-comparisons. Advantages or drawbacks of explicit and implicit models have to be made clear, in particular the representation of dominant processes in the studied area by different approaches. This would increase the credibility of present results; otherwise criticism would not be justified.*

The only other unstructured grid modelling study investigating the TSS together with the Black Sea by Stanev et al. (2017) considers the entire region in the same model domain, but both the resolution and the number of computational nodes are essentially much less than ours, the topography also being not well represented. The study manages to arrive to few results that seem to be in line with our own conclusions on the coupled behaviour of the TSS, although the focus of the paper is more on the intrusion of the Bosphorus inflow into the Black Sea, rather than the specifics of the TSS. Therefore there is not much to be discussed with respect to specific features of the models.

A further unstructured grid model was recently presented by Ferrarin et al. (2018) after our submission of the present paper, studying the tidal dynamics in the inter-connected Black Sea – Mediterranean Sea system. We now mention their study in the introduction section, although there is no possibility of inter-comparison.

*c) Analyze, in a quantitative way, processes in the straits and the skill of model to replicate the basic physics. There your model is superior in comparison with the structured grid ones and you need to demonstrate this.*

The reviewer is quite right in stating the superiority of the present model. The absolute requirement to represent extreme physical processes of the TSS at the finest scale possible in a model of the region has been the main motivation on our part to select a full-featured hydrodynamic model of unstructured genre. In addition, the need to represent all of the possible strait processes in full had been demonstrated by earlier studies by Sözer and Özsoy (2017) and the need to represent the straits as well as the Marmara Sea and the adjacent basins in fine detail in a model of the whole region had been found to have a central importance in Sannino et al. (2017). Essentially, it has been shown that the ‘systems behaviour’ of the model of the whole TSS behaves much differently from a linear extension of the results from models of its individual parts. Despite these considerations of dissimilarity, we further qualitatively compare our results with Sözer and Özsoy (2017) in section 3.3 to show that the main features found in the stand-alone strait model are adequately represented in normal and extreme situations. Perhaps the only missing part is the detailed comparison with the behaviour of the Dardanelles Strait, although that probably has to wait for a full-fledged investigation of the strait hydrodynamics by a stand-alone model. These motivations and the main results of former studies as applied to the present study have been quite transparently discussed in the introduction section and throughout the paper.

*2. One sea forced by two straits presents a very interesting system to explore salt and mass balances and the role of straits for the water mass formation, in particular. This issue is only marginally addressed. Analysis is not very symmetric; more attention has been given to the Bosphorus. One would like to see a figure similar to Fig. 12 for the Dardanelles. This is very important because the latter provides the source of deep water masses (see Fig. 6b; why is this figure cut at 100m?). The analysis of Fig 6 and associated processes needs to be extended down to the depth of the maximum reach of Aegean Sea water. It could be that the trend in Fig. 7 reflects a trend in the deep waters (or a problem with initialization). These comments lead me to the conclusion that authors have to deepen the physical interpretation of their results.*

As this paper is not dedicated to water mass formation analysis but to a novel understanding of the role played by atmospheric and water fluxes forcing on the TSS circulation, we only interpret what we observe in the model results as regards water masses and prefer to reserve to address details of water mass formation processes for future studies. We should also like to express our private view on the practicality of such analysis at this stage: the rather demanding nature of the model runs and the post-processing in terms of high performance computing and storage capacity has been a deterrent to have repeated scenario runs that would be needed for water mass analyses.

The asymmetry in the analysis towards Bosphorus is not only because historically more is known about this Strait, but also because the Bosphorus is the more strictly limiting member of the TSS as a result of its rather special “maximal exchange” hydraulic regime, as demonstrated by recent modelling results by Sözer and Özsoy (2017) and Sannino et al. (2017). The role of the larger Dardanelles Strait is also important, and should be further investigated to reveal its different hydraulic regime and role in the overall system behaviour.

We provide the same figure (now Fig. 13 in the marked-up version) for the Dardanelles as Fig.12 of the Bosphorus and discuss it in section 3.3. Very briefly, the layered-structure of the water column in normal conditions in Nov. 15, 2008 (Fig.13a) resembles the case of Sannino et al. (2017, Fig. 7). In Nov. 22, 2008, as a result of the more active atmospheric conditions, the salinity in the upper layer increases by extensive mixing. Further, the stratification is broken partially in the Marmara Sea side of the strait. The structure of the two-layered flow and response of the model to the atmospheric events seems correct.

We note that the trend in Fig. 7 is due to the initialization. The initial fields are obtained from a lock-exchange simulation started from three different vertical profiles for each of the Black, Marmara and Aegean Seas as explained in section 2. We can deduce that the profiles chosen to initialize Marmara Sea is warm and the simulated volume mean temperature gradually gets cooler until 2012 with the intrusion of the Aegean Sea water. In Fig. 6, we showed only the first 100 m. before since our analysis is focused on the upper layer structures interaction with the atmospheric forcing. However, we now provide the figure extended down to 600 m. We discuss this issue in the section 3.2 of the revised manuscript.

*3. Some of the presented results could reveal that the mass and salt balance in the model is not correctly represented. This is a fundamental issue, which could convey very negative misinterpretation of FESOM skills. Net water transport in Bosphorus, as seen in Tabl. 4, is  $\sim 150\text{km}^3/\text{yr}$ ; in the Dardanelles it is  $\sim 100\text{km}^3/\text{yr}$ . This is in contradiction with the net transport published earlier by one of the authors (Özsoy and Unluata, 1997, their Fig. 5) where it was shown that the water flux at the Marmara air- sea interface is minor in comparison to the straits transport. Results in Table 4 are also in contradiction with the statement “The resulting net water flux  $P - E$  varies between  $-4.7 \times 10^{-8}$  and  $2.5 \times 10^{-8}$  m/s.” Taking the area of Marmara Sea  $\sim 11.000 \text{ km}^2$  and looking in Fig. 3 where the mean water flux is  $\sim -1 \times 10^{-8}$  m/s yields also a negligible water flux at the Marmara Sea surface. Authors have to look closely how to explain the difference between  $\sim 150\text{km}^3/\text{yr}$  and  $\sim 100\text{km}^3/\text{yr}$ . They have to carefully check the conservation of mass and tracers and include this, if they submit a*

*new manuscript. Unlike the models with large open boundaries, the Marmara Sea gives unique opportunities to address conservation properties and authors have to take advantage of it.*

We thank a lot to the reviewer for drawing our attention to volume transports, which appeared inconsistent in the earlier manuscript. A similar issue has been pointed out by reviewer #1 for the Bosphorus Strait. We discuss the problem in full details here, update and provide corrected estimates of fluxes.

The major problem with the volume transport computations was that they were based on daily snapshots rather than daily averages of the current velocity data in the model outputs. We have now corrected and documented the estimates in Table 4 and Fig. 14 (please see the marked-up version of the manuscript below).

Secondly, as our implementation of the TSS model has closed lateral boundaries we needed to have the net water flux over the domain to be zero at each time step. Our choice to satisfy this requirement is to take out the excess water volume flux that arises at every time step and distribute it over the model domain in order to act as a surface flux correction. This is also the solution used by Gent et al., (1998) as well as all the global implementations of FESOM referred in the manuscript. (Please see other considerations in the reply to Reviewer #1).

However, one of the drawbacks of our choice is the one pointed out by the reviewer. The volume flux entering into the Straits has already been partly taken out from the surface by  $W_{\text{corr}}$  term in equation (A9). This explains also why the barotropic fluxes in the Straits are gradually decreasing throughout the TSS from northern Bosphorus to southern Dardanelles sections.

More specifically, Fig.3 which shows the water fluxes in the Marmara Sea now includes also the correction term  $W_{\text{corr}}$  in Fig.3b in the revised version. A similar figure for the whole domain is also provided in Fig.3a. For the whole domain, the mean runoff is  $287 \text{ km}^3/\text{yr}$  in the Black Sea buffer zone with seasonal variability. The total mean evaporation and precipitation are  $-131.5$  and  $70.8 \text{ km}^3/\text{yr}$ , respectively (positive into the ocean). Their sum is  $226.4 \text{ km}^3/\text{yr}$  which is the mean water flux correction to conserve volume over the whole domain.

As discussed in the Appendix B, we distribute this correction to the whole surface, weighted by the area of each sub-region (please see Table A which now includes area of different compartments of the TSS). The mean correction applied in the Marmara Sea is, therefore,  $-15.9 \text{ km}^3/\text{yr}$  (Fig. 3b). The net outflux is  $-17.1 \text{ km}^3/\text{yr}$  including evaporation minus precipitation.

Given the net volume transports through the southern Bosphorus and northern Dardanelles as  $-150.0$  and  $-132.8 \text{ km}^3/\text{yr}$ , the difference between the two lateral boundaries of the Marmara Sea is  $-17.2 \text{ km}^3/\text{yr}$  which is balanced by the surface water flux. The surplus is  $0.1 \text{ km}^3/\text{yr}$ , which is less than 0.1% of the volume transport through the southern Bosphorus transect. This small numerical error could originate from the transport computation which approximates the fluxes through the fully-shaved cells at the bottom boundary layer. The transport difference between the two ends of the Dardanelles is

slightly higher possibly because of the increased evaporation at the wide section off the Strait and the deep channel topography on one side of an otherwise flat topography at the exit region also being liable to errors in flux computations. Overall, the errors are negligible and the budgets computed separately for each component of the TSS are closed, verifying continuity in the average transports through the system.

*4. A further problem is identified in the comparison between Table 4 and Table 5 demonstrating that water flowing through the strait of Bosphorus is two times less than what is reported in the literature ( $\sim 300 \text{ km}^3/\text{yr}$ ). There are two problems here.*

None of the estimates in Table 5, except Kanarska and Maderich (2008), is a numerical simulation. All of the estimations are done using mass conservation by assuming an E-P-R=300 km<sup>3</sup>/yr in the Black Sea. We provide it to the model as we have shown in our response to the comment #3. However, our choice of correction in our modelling approach reduces the fluxes approximately 50 % and we know how to correct it. We note that modeling study of Kanarska and Maderich (2008) also computes less net transport compared to other estimates which is possible in numerical models. All of the computations are only estimates. Here, in our first try, what is important for us is to show that the water fluxes are balanced to conserve average properties in the closed domain used. In our further studies, we intend to improve the solution, by applying the water flux correction finally to a water flux sink that takes out the residual water flux after accounting for the total E-P-R in the system and adding to it any corrections tightly balancing the water budget. (see further comments provided in response to Reviewer #1).

*a) I wonder how with  $\sim$ two times smaller net transport authors simulate realistically the two layer transport and its impact on the Marmara Sea circulation. What about the deep layer transport in the Dardanelles? Isn't there a trend in the system if you have unrealistic fluxes in the straits (see Fig. 7b)?*

There is no trend in the system as can be seen from Fig. 11 for the sea level and Fig. 13 (now Fig.14 in the marked-up version) for the volume transports. It is the correction term  $W_{\text{corr}}$  in equation (A9) that reduces the volume transport along the way from the Black Sea to the Aegean Sea. Further care is given to stress the important role of the volume and mass conservation in a closed lateral boundary models. In fact, the purpose of the whole flux correction procedure is to satisfy conservation in the closed basin model, and that strategy has worked, albeit some relatively simple choice, to prevent physically and numerically based trends in the simulations.

*b) Two times smaller net transport means that the fresh water balance in the Black sea is wrong. Led by these arguments, I again propose that authors present clearly the model forcing at all open boundaries, rivers and air-sea interface, as well as and the corresponding fresh water and salt balances for the Black Sea, Aegean Sea and Marmara Sea.*

There is no imbalance or trend due to the water fluxes in the system, we have clarified the role of the correction term and its impact on the net transports in comments 3 and 4. We decided to use the approach which maintained a reasonable salinity difference between the Aegean and the Marmara Sea. Another possible solution is to use an Aegean Sea buffer zone to balance the Black Sea net water flux due to runoff. This means that all the extra runoff from the Black Sea would be compensated in the

Aegean. This is the strategy used by Tonani et al. (2008) for the Mediterranean Sea and tested in this model domain by Gürses et al. (2016).

## References

Gent, P. R., Bryan, F. O., Danabasoglu, G., Doney, S. C., Holland, W. R., Large, W. G., & McWilliams, J. C. (1998). The NCAR climate system model global ocean component. *Journal of Climate*, *11*(6), 1287-1306.

Kanarska, Y. and Maderich, V.: Modelling of seasonal exchange flows through the Dardanelles Strait, *Estuarine, Coastal and Shelf Science*, *79*, 449–458, 2008.

## Author' response to RC#3

### Major comments

*However, it is necessary to discuss the result from the validation, showing that the model error increases in time (Table 2). From Figure 7 it is seen the negative trend in the volume temperature and positive for the volume salinity, what could be the reason for this trend?*

The reason for the trend is the chosen initial condition in the Aegean Sea. It takes about four years in Marmara Sea to reach statistical stability when we initialize the model from horizontally uniform initial conditions. The negative trend for temperature is connected to the heat flux forcing while the salinity to the water flux forcing.

*The section on the sea level and mass transport in the straits is also interesting. Figure 11 does not quite clear show what is the correlation between observations and simulations.*

The correlation between the observed and simulated sea level differences is computed as 0.56. We will include it in the revised manuscript.

*There is information on the lower and upper layer velocity, but it is advisable to give more details on the variability of the interface depth.*

We provided some information for the spatial variability of the interface depth in different strait junctions in Table 3 of the manuscript.

*The chapter on Marmara Sea dynamics is well written. Figure 15 and 17 might look better in color as Figure 16.*

Thanks. We prefer to keep the figures as they are since we want to put emphasis on contours and vectors.

### Some concrete remarks:

*-The terms for  $\alpha$  and  $\beta$  are thermal expansion and haline contraction coefficients, their values might be also given in the table with parameters.*

They are computed in the model following *McDougall, T. J. (1987). Neutral surfaces. Journal of Physical Oceanography, 17(11), 1950-1964.* We include the reference in the revised version with an explanation.

*- The Figure 3 could be also in colors, now it is not very well read.*

Thanks, we provided a colored version of the Fig. 3.

*- Figure 6b shows cooling on the surface at the south end of Bosphorus, is it realistic?*

We think it is possible by surfacing of the cold tongue following the hydraulic jump due to the control exerted by the contraction in the Bosphorus may lead such an anomalous spots in the entrance of the Marmara Sea.

*-There is an unfinished sentence with ??????*

Thanks, the sentence is correct after removing the question marks. It is a typo after compilation by latex.

#### References

McDougall, T. J.: Neutral surfaces, *Journal of Physical Oceanography*, 17, 1950–1964, 1987.

## Author' response to SC#1

We thank Dr. Zhang for their interest to our study. We also appreciate his contribution during interactive discussion and giving us the opportunity to discuss further the study presented in Stanev et al. (2017). Below is our response to SC1 by Dr. Zhang.

*1. The criticism of the paper of Stanev et al. (2017) is mostly off the mark. Below are their texts: ' Stanev et al. (2017) used an implicit advection scheme for transport to handle a wide range of Courant numbers (Zhang et al., 2016) while satisfying the stability of the solution. However, the computational burden of using an implicit scheme imposed a coarser model resolution with 53 vertical levels at the deepest point of the Black Sea. I note that this limitation may, particularly in the Bosphorus, lead to excessive vertical mixing or a widened interface thickness, which are crucial for the intrusion of the Mediterranean origin water into the Black Sea. This can be seen in their Figures 11c and 11d, for example.'*

*I want to bring to the attention of authors that: a) 53 vertical levels in the Bosphorus, which in some places is ~30 m deep, is less than 1 m vertical resolution with the used vertical coordinates, that is better than the resolution used by authors. They say "The vertical resolution is 1 m in the first 50 m". The conclusion is that authors have to spend some time to reading carefully what other scientist have published. b) SCHISM uses explicit Eulerian-Lagrangian approach for momentum advection (which is unconditionally stable). It also uses an implicit scheme for terms in the momentum and continuity equations that place most stability constraints (pressure gradient, divergence, vertical viscosity). Most importantly, the size of matrix from the implicit scheme is determined by number of horizontal nodes, not this times number of levels. In fact we have used 92 levels in one version of our Kuroshio simulation and it went fine. So it's not a fundamental problem for us to use a large number of levels - it's just a practical consideration given our limited computational resource (see also my comment (a)). In any case, your results inspired us to try larger number of levels in the future.*

*Our experience with our own and other Z-coordinate models is that it requires a large number of levels to get reasonable stratification and bottom intrusion right (due to stair- case). We switched to hybrid coordinates precisely because of this. I hope that authors will avoid conveying this kind of mis-information.*

1-a) Here, Dr. Zhang mentioned our interpretation on the vertical discretization used in Stanev et al. (2017). As quoted by Dr. Zhang, we said "However, the computational burden of using an implicit scheme imposed a coarser model resolution with 53 vertical levels at the deepest point of the Black Sea". Dr. Zhang responded as "53 vertical levels in the Bosphorus, which in some places is ~30 m deep, is less than 1 m vertical resolution with the used vertical coordinates, that is better than the resolution used by authors." Here, we note that Stanev et al. (2017) states the 53 vertical levels in the deepest part of the Black Sea, not in the Bosphorus as claimed by Dr. Zhang. The exact phrase that is written in Stanev et al. (2017) is (in section 3.1 paragraph 3): "The vertical LSC2 grid consists of up to 53 levels in the deepest parts of the Black Sea, with an average number of 31.65 levels in the whole model domain." Our interpretation is that relatively shallow areas in the model domain (we assume Azov Sea, Bosphorus and other straits since it is not explicitly mentioned by the authors) should have even less

than 31.65 levels to have it as an average number. Therefore, we have difficulty to understand when Dr. Zhang claims that Stanev et al. (2017) has higher vertical resolution than our model has. We would appreciate if they could have been clearer in their paper. We kindly ask Dr. Zhang to clarify the point if we miss anything and have to modify our interpretation. Finally, we are happy that Dr. Zhang confirms us by saying “our own and other Z-coordinate models is that it requires a large number of levels to get reasonable stratification” but afraid that the mentioned requirement is not satisfied by Stanev et al. (2017), especially in the straits.

1-b) We are happy with the work presented in Stanev et al. (2017) since they show the capabilities of the unstructured meshes in modeling the Turkish Straits System. We appreciate their efforts in using implicit scheme for time discretization since explicit schemes has very strict CFL limitations as we discussed in the manuscript. However, although we don't claim of being experts on implicit schemes, we would prefer to see some discussion in Stanev et al. (2017), on the accuracy as they did on the stability since we know that accuracy of the solution can be degraded when implicit schemes are used especially in very dynamic regimes as in Bosphorus. Moreover, besides not having fully understand the relation of Stanev et al. 2017 with their work on Kuroshio current, Dr. Zhang admits the computational cost of using implicit schemes and as a result they kept the vertical resolution lower than needed in Stanev et al. (2017) as we concluded. According to us, this is a crucial mistake in modelling especially the Bosphorus Strait. Because of the same challenge, we preferred to increase the vertical resolution rather than including all the Black Sea as we proposed in our conclusions and performed by Stanev et al. (2017). Although their hybrid LSC2 grid allows to increase the resolution at the surface and the bottom, we think that they missed a lot around the interface between the upper and lower layers. The strong mixing, probably due to the diffusion, can be seen from their Fig. 5c , quite easily. If they are interested to see a better representation of the interface, they can have a look at Fig. 12 or Fig. 8 of Sannino et al. 2017 in the models and Figure 4 of Gregg et al. (1999) from the observations.

*2. I expected, after having seen their wrong criticism against the work of Stanev et al. (2017), to see some examples. Unfortunately, this paper is only cited in the introduction, so their statement there is totally unjustified. A fair approach would be to clearly demonstrate what their progress is in comparison with earlier unstructured-grid experiments.*

2) Stanev et al. (2017) focuses on the Black Sea by resolving also the Turkish Straits System. However, our main focus is the Marmara Sea which is barely analyzed in Stanev et al. (2017). Therefore, we don't see any reason to make any comparison as we did, for example, with Sannino et al. (2017) which has a focus similar to us. However, we are happy to refer Stanev et al. (2017) in the introduction being aware that studies on the Turkish Straits System attract more and more attention.

## References

Sannino, G., Sözer, A., and Özsoy, E.: A high-resolution modelling study of the Turkish Straits System, *Ocean Dynamics*, 67, 397–432, <https://doi.org/10.1007/s10236-017-1039-2>, 2017.

Gregg, M. C., Özsoy, E., & Latif, M. A. (1999). Quasi-steady exchange flow in the Bosphorus.

Geophysical Research Letters, 26(1), 83-86.

## Author' response to SC#2

*My major concern with this study is on the capability of the present model application to correctly reproduce the water circulation in the system and the exchange dynamics at the Dardanelles and Bosphorus straits. The authors argue in the abstract and in the results description that the simulation maintains its realism. However, the evidences provided in the paper demonstrate that some numerical model results are unrealistic.*

We do not have a claim that we model every aspect of the TSS with very high accuracy. Here, what we present for the first time is a long-term simulation of the system and analysis of the evolution of the system under realistic atmosphere. Since it is done for the first time, we do not understand how Dr. Ferrarin reached a conclusion that some results are unrealistic.

*In particular: - The water fluxes presented in the table 4 are about half than what is reported in the literature (Table 5).*

We discuss the issue extensively in our response to the comment #3 of the Reviewer #2.

*- The water fluxes presented in Figure 13 do not reproduce the observed variability and magnitude.*

We discuss the issue extensively in our response to the comment #3 of the Reviewer #2.

*- The thermocline and halocline are generally deeper than what is observed (Figure 9).*

That is something that we mention when we discuss higher RMS errors around the pycnocline. Although different factors such as the insufficient variability of the Bosphorus inflow, coarse resolution of atmospheric forcing may be the reasons, we want to stress that the profiles in Fig. 9 are the mean of a couple of days and it is difficult to reproduce exactly the same profiles without any data assimilation.

*- The numerical model seems not able to correctly reproduce the observed sea level differences between Yalova and Sile. The authors should provide statistics (RMSE, BIAS, R2) of the model performance for the water levels.*

We think the model is capable of reproducing the sea level difference as much as the atmospheric forcing permits. We believe the solution will substantially improve with a higher resolution atmospheric forcing, which can only be provided by a regional model, currently.

*Concluding, to my opinion, the authors have to provide clear and robust calibration and validation of their numerical model application before inferring on the water circulation of the Turkish Strait System.*

# Circulation of the Turkish Straits System ~~between 2008-2013~~ under complete interannual atmospheric forcings

Ali Aydođdu<sup>1,2,3</sup>, Nadia Pinardi<sup>2,4</sup>, Emin Özsoy<sup>5,6</sup>, Gokhan Danabasoglu<sup>7</sup>, Özgür Gürses<sup>5,8</sup>, and Alicia Karspeck<sup>7</sup>

<sup>1</sup>Science and Management of Climate Change, Ca' Foscari University of Venice, Italy

<sup>2</sup>Centro Euro-Mediterraneo sui Cambiamenti Climatici, Bologna, Italy

<sup>3</sup>Nansen Environmental and Remote Sensing Center, Bergen, Norway

<sup>4</sup>Department of Physics and Astronomy, University of Bologna, Italy

<sup>5</sup>Institute of Marine Sciences, Middle East Technical University, Erdemli, Turkey

<sup>6</sup>Eurasia Institute of Earth Sciences, Istanbul Technical University, Turkey

<sup>7</sup>National Center for Atmospheric Research, Boulder, Colorado

<sup>8</sup>Alfred Wegener Institute for Polar and Marine Research, Bremerhaven, Germany

**Correspondence:** Ali Aydođdu (ali.aydogdu@nersc.no)

**Abstract.** A simulation of the Turkish Straits System (TSS) using a high-resolution, three-dimensional, unstructured mesh ocean circulation model with realistic atmospheric forcing for the 2008-2013 period is presented. The depth of the interface layer-pycnocline between the upper and lower layers remains stationary after six years of integration, indicating that despite the limitations of the modelling system, the simulation maintains its realism. The solutions capture important responses to high frequency atmospheric events such as the reversal of the upper layer flow in the Bosphorus due to southerly severe storms, i.e., blocking events, to the extent that such storms are present in the forcing dataset. The annual average circulations show two distinct patterns in the Marmara Sea. When the wind stress maximum is localised in the central basin, the Bosphorus jet flows to the south and turns west after reaching the Bozburun Peninsula. In contrast, when the wind stress maximum increases and expands in the north-south direction, the jet deviates to the west before reaching the southern coast and forms a cyclonic gyre in the central basin. In certain years the mean kinetic energy in the northern Marmara Sea is found to be comparable to that of the Bosphorus inflow.

## 1 Introduction

The Turkish Straits System (TSS) connects the Marmara, Black and Mediterranean Seas through the Bosphorus and Dardanelles Straits. The near-surface layer of low salinity waters originating from the Black Sea enters from the Bosphorus, flowing west and exiting into the Aegean Sea at the Dardanelles. The deeper, more saline waters of Mediterranean origin enter from the Dardanelles in the lower layer and eventually reach the Black Sea through the undercurrent of the Bosphorus. The strongly stratified marine environment of the TSS is characterised by a sharp pycnocline positioned at a depth of 25 m (Ünlüata et al., 1990). The complex topography of the Marmara Sea consists of a wide shelf in the south, a narrower one along the north-

ern coast and three east-west deep basins separated by sills, connected to the two shallow, elongated narrow straits providing passage to the adjacent seas at the two ends, as shown in Fig. 1.

The TSS mass and property balances are mainly controlled by the Black Sea in the upstream. At the Bosphorus Black Sea entrance, the long-term salinity budget implies a ratio of about two between the upper and lower layer volume fluxes (Peneva et al., 2001; Kara et al., 2008). The net flux is estimated to be comparable to the Black Sea river runoff, as the annual average precipitation and evaporation over the sea surface are roughly of the same order (Özsoy and Ünlüata, 1997). Daily to seasonal variations in net fluxes through the TSS are driven by changes in Black Sea river runoffs, barometric pressure and wind forcing.

Climatological means of water and tracer fluxes through the TSS were initially estimated from long-term observations of seawater properties at junctions of the straits and on surface water fluxes (Ünlüata et al., 1990; Beşiktepe et al., 1994; Tuğrul et al., 2002; Maderich et al., 2015), followed later by ship-borne and moored ADCP measurements at the straits (Özsoy et al., 1988; Özsoy et al., 1998; Altıok et al., 2012; Jarosz et al., 2011b, a, 2012, 2013). Updated reviews of TSS fluxes based on combined data have been provided by Schroeder et al. (2012); Özsoy and Altıok (2016); Sannino et al. (2017); Jordá et al. (2017).

The hydrodynamic processes of the TSS extend over a wide range of interacting space and time scales. The complex topography of the straits and property distributions have resulted in hydraulic controls being anticipated in both straits (Özsoy et al., 1998; Özsoy et al., 2001), which can only partially be demonstrated by measurements at the northern sill of the Bosphorus (Gregg and Özsoy, 2002; Dorrell et al., 2016). Hydraulic controls have since been found by modelling at the southern contraction-sill complex and the northern sill, confirming a unique maximal exchange regime adjusted to the particular topography and stratification (Sözer and Özsoy, 2017a; Sannino et al., 2017). These findings support the notion that the Bosphorus is the more restrictive of the two straits in controlling the outflow from the Black Sea to the Mediterranean. The analysis of moored measurements by Book et al. (2014) demonstrated this, and indicated a more restrained sea level response transmitted across the Bosphorus than in the Dardanelles.

Improvements in modelling have provided a better scientific understanding of the TSS circulation, and they can now address the complex processes characterising the system. The initial step in this formidable task is to construct separate models of the individual compartments of the system, which are the two Straits and the Marmara basin. The first simplified models of the Bosphorus were by Johns and Oğuz (1989) who solved the turbulent transport equations in 2D, and found a two-layer stratification to develop. Simplified two-layer or laterally averaged models of the Dardanelles and Bosphorus were later developed by Oğuz and Sur (1989), Stashchuk and Hutter (2001) and Oğuz et al. (1990) respectively, while Hüsrevoğlu (1998) introduced a 2D reduced gravity ocean model of the Dardanelles inflow into the Marmara Sea. Similar 2D laterally averaged models (Maderich and Konstantinov, 2002; Ilıcak et al., 2009; Maderich et al., 2015) and 3D models (Kanarska and Maderich, 2008; Öztürk et al., 2012), which were of limited extent, have been used to construct simplified solutions for the Bosphorus exchange flows. Bosphorus hydrodynamics were extensively investigated by Sözer and Özsoy (2017a) using a 3D model with turbulence parameterisation under idealised and realistic topography with stratified boundary conditions in adjacent basins, demonstrating the unique hydraulic controls in the maximal exchange regime that are to be established in the realistic case. The combined effects of the Bosphorus and the proposed parallel channel known as Kanal İstanbul have been investigated by

Sözer and Özsoy (2017b), indicating weak coupling between the two channels, which have very different characteristics, but this has been found to be of climatic significance in modifying the fluxes across the TSS.

Very few studies have attempted to model the circulation in the Marmara Sea, even as a stand-alone system excluding the dynamical influences of the straits and atmospheric forcing. Chiggiato et al. (2012) modelled the Marmara Sea using realistic atmospheric forcing and open boundaries at the junctions of the straits with the Sea, indicating surface circulation changes in response to changes in the strength and directional pattern of the wind force.

Similarly, the interannual variability of the Marmara Sea has been examined by Demyshev et al. (2012) using open boundary conditions at the strait junctions in the absence of atmospheric forcing. They reproduced the S-shaped jet current traversing the basin under the isolated conditions of a net barotropic current, which with appropriate parameterisation successfully preserved the sharp interface between the upper and lower layers when the model steady-state was reached after 18 years of simulation. The S-shaped upper layer circulation of the Marmara Sea predicted by Demyshev et al. (2012) appears similar to what Beşiktepe et al. (1994) found in summer, when wind forcing is at its minimum or at least close to being in a steady-state. An anti-cyclonic pattern has generally been identified in the central Marmara Sea, like the cases reported by Beşiktepe et al. (1994).

The challenges of modelling the entire TSS domain were recently undertaken by Gürses et al. (2016). The effects of atmospheric forcing were considered, excluding the effects of the net flux through the TSS. The study used an unstructured triangular mesh model, the Finite Element Sea-Ice Ocean Model (FESOM), with a high horizontal resolution reaching about 65 m in the straits in the horizontal. The water column is discretized by 110 vertical levels.

The study of Sannino et al. (2017) used curvilinear coordinate implementation of the MITgcm (Marshall et al., 1997) with a non-uniform grid in the horizontal, a minimum of 65 m resolution in the narrowest part of Bosphorus and 100 levels in the vertical. The model was used to investigate the circulation of the TSS under varying barotropic flow through the system in the absence of atmospheric forcing. The overall circulation in the Marmara Sea was found to differ significantly [in each of their experiments](#) with variations in the net volume transport at the Bosphorus. The circulation changes from a large anticyclonic circulation at the centre of the basin at low flux values, to different gyres wrapped around an S-shaped jet as the net flux is increased. A cyclonic central gyre is eventually generated as the increased flux leads to the lower layer in the Bosphorus being blocked. The most significant finding was the nonlinear sea level response, which deviated widely from the linear response predicted by the stand-alone Bosphorus model of Sözer and Özsoy (2017a).

Stanev et al. (2017) approached the challenge by using an unstructured mesh model. The model covers the entire Black Sea, and is seamlessly linked to the TSS and the northern Aegean Sea with open boundaries in the south and uses realistic atmospheric forcing. The focus is on the transport at the straits and the resulting dynamics of the Black Sea. Regarding the TSS, the results support the notion of multiple controls of the barotropic flow. They were also able to simulate short-term events such as severe storm passages. However, in a high-resolution model of the TSS, the Courant-Friedrichs-Lewy (CFL) condition (Courant et al., 1967) restricts the time step to a few seconds with explicit schemes. As a solution, Stanev et al. (2017) used an implicit advection scheme for transport to handle a wide range of Courant numbers (Zhang et al., 2016) while satisfying the stability of the solution. However, the computational burden of using an implicit scheme imposed a coarser model resolution

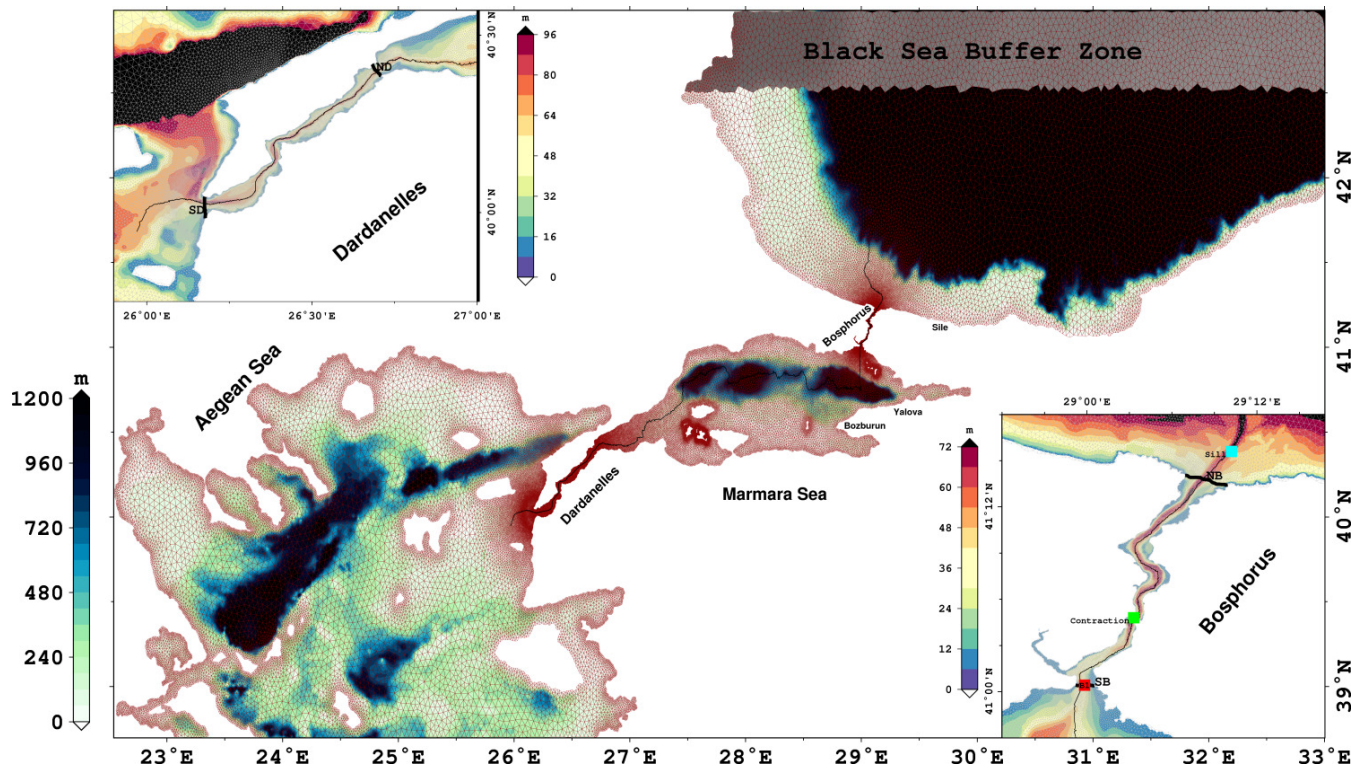


**Figure 1.** Bathymetry of the Turkish Straits System and the [whole](#) model domain. Bathymetry of the Bosphorus and Dardanelles Straits are detailed in the small panels. The colours represent the depth. The colourbar scales are different for the straits and the whole domain. A triangular mesh is overlaid with red for the entire domain and with grey for the straits in small panels. The Thalweg used to display the cross-section throughout the TSS is represented by the black line. The grey shaded area in the Black Sea functions as a buffer zone and is described in the text. Cross-sections at the boundaries of the straits are used for volume flux computations. NB, SB, ND and SD in the small panels are northern Bosphorus, southern Bosphorus, northern Dardanelles and southern Dardanelles, respectively. In the Bosphorus panel, the green and cyan squares show the locations of the contraction and northern sill, respectively. Finally, the red square B1 indicates the middle of the Marmara Sea exit of the Bosphorus Strait.

with 53 vertical levels at the deepest point of the Black Sea. We note that this limitation may, particularly in the Bosphorus, lead to excessive vertical mixing or a widened interface thickness, which are crucial for the intrusion of the Mediterranean origin water into the Black Sea. This can be seen in their Figures 11c and 11d, for example.

5 [Another recent study by Ferrarin et al. \(2018\) presents the tidal dynamics in the TSS which is seamlessly included in a model domain covering whole Black Sea - Mediterranean system. They use a barotropic version of the SHYFEM \(Umgiesser, 2012\) to provide the hydrodynamical background to the tidal analysis.](#)

In our work, we simulate the complete TSS system with a high vertical resolution unstructured grid model forced by complete heat, water and momentum fluxes. A long-term six-year simulation is used to analyse the combined response of the Marmara Sea to atmospheric forcing and strait dynamics. The questions addressed in this paper are: What is the mean Marmara Sea circulation and its variability in a long-term simulation? What are the effects of the atmospheric forcing on the Marmara Sea dynamics and circulation?

10

The paper is organised as follows: In the next section, we document the model setup and the details of the experiment. In section 3, the validation of the water mass structure and sea level differences along the TSS are demonstrated. The resulting volume transports through the straits, and the kinetic energy and circulation in the Marmara Sea, are presented. Finally, in section 4, we summarise and discuss the results.

## 5 2 Model Setup

Models for solving the dynamical equations for an unstructured mesh using finite element or finite volume methods have been implemented for many idealistic applications (White et al., 2008; Ford et al., 2004), and in realistic coastal ocean studies (Zhang et al., 2016; Federico et al., 2017; Stanev et al., 2017). An obvious advantage of using an unstructured mesh model is the varying resolution, which allows for a finer mesh resolution in coastal areas than in the open ocean. The general ocean circulation model used in this study is the Finite Element Sea-ice Ocean Model (FESOM). FESOM is an unstructured mesh ocean model using finite element methods to solve hydrostatic primitive equations with the Boussinesq approximation (Danilov et al., 2004; Wang et al., 2008). We use the initial implementation of Gürses et al. (2016).

The model domain extends zonally from 22.5°E to 33°E and meridionally from 38.7°N to 43°N, covering a total surface area of  $1.52 \times 10^{11} \text{ m}^2$  (Fig. 1). The mesh resolution is as fine as 65 m in the Bosphorus and 150 m in the Dardanelles. In the Marmara Sea, the resolution is always finer than 1.6 km and is not coarser than 5 km in the Black Sea and the Aegean Sea. The water column is discretized by 110 vertical z-levels. The vertical resolution is 1 m in the first 50 m depth and increases to 65 m at the bottom boundary layer in the deepest part of the model domain.

Model equations and parameters are documented in appendix A. The current model implementation considers closed lateral boundaries. Therefore, volume and salinity conservations are imposed to prevent drifts in the tracer fields. Our approach for volume and salinity conservations is described in appendix B.

The experiment detailed below was conducted over six years, commencing on 1 January 2008 and continuing until 31 December 2013. The initial fields were obtained after a three-month integration of a lock-exchange case, which was initialised from different temperature and salinity profiles in the basins of the Black, Marmara and Aegean Seas (Gürses et al., 2016; Sannino et al., 2017). Fine mesh resolution and energetic flow structures in the straits require small time steps so the CFL condition is not violated. The time step is thus set to 12 s throughout the integration. The simulation was forced by atmospheric fields provided by ECMWF with  $1/8^\circ$  resolution. The forcing data cover the whole experiment period with a time frequency of six hours. Precipitation data are obtained from monthly CPC Merged Analysis of Precipitation (CMAP, Xie and Arkin (1997)) and interpolated to the ECMWF grid as daily climatology.

The annual mean of wind, wind stress and wind stress curl for the simulation period are shown in Fig. 2. Wind stress,  $\tau$ , is calculated as

$$\tau = \rho_0 C_d |\mathbf{u}_{wind}| \mathbf{u}_{wind} \quad (1)$$

where  $C_d$  is the drag coefficient and  $\mathbf{u}_{wind}$  is the wind velocity. The annual mean wind fields are northeasterlies which were strongest in 2011.  $\tau$  was higher than  $0.04 \text{ Nm}^{-2}$  in the central-north Marmara Sea in 2009. It then expands in a north-south

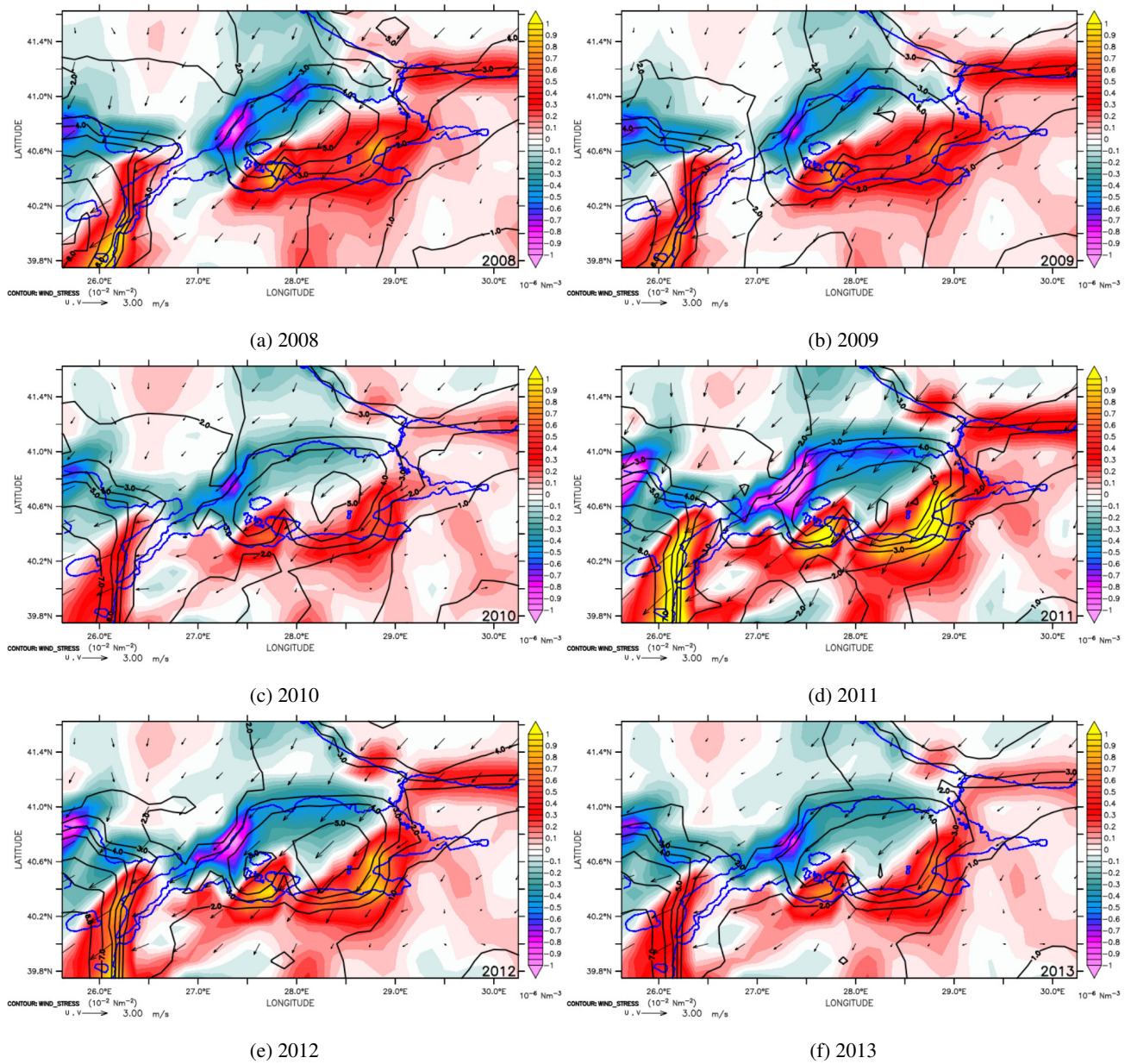


**Figure 2.** Annual mean of wind velocity ( $\text{ms}^{-1}$ , arrows), wind stress ( $10^{-2}\text{Nm}^{-2}$ , black contours) and wind stress curl ( $10^{-6}\text{Nm}^{-3}$ , shades) in the Marmara Sea for each year from 2008 (top left) to 2013 (bottom right). The coastline is overlaid in blue.

direction, exceeding  $0.05 \text{ Nm}^{-2}$  in the central basin, in 2011 and then weakens again in 2013. The wind stress curl is a dipole shaped by the northeasterlies and is negative in the north and west, and positive in the south and east of the Marmara Sea. In 2011, the wind stress curl in the coastal zones was more intense than in the other years.

Month	Jan	Feb	Mar	Apr	May	Jun
$R(km^3/yr)$	260.3	281.7	333.9	404.1	417.6	353.6
$S^*(psu)$	18.97	18.96	18.91	18.88	18.74	18.74
Month	Jul	Aug	Sep	Oct	Nov	Dec
$R(km^3/yr)$	292.5	231.2	198.7	196.2	223.0	254.2
$S^*(psu)$	18.87	18.98	18.90	18.92	18.94	19.02

**Table 1.** Monthly Black Sea river discharges ( $R$ ) and salinity relaxation values ( $S^*$ ).

A surface area of  $2.22 \times 10^{10} \text{ m}^2$  north of  $42.5^\circ\text{N}$  in the Black Sea functions as a buffer zone (the grey shaded area in Fig. 1). This zone is utilised to provide required water fluxes for a realistic barotropic flow through the Bosphorus. The model is forced by a climatological runoff in the Black Sea, which is essential to generate realistic sea level differences between the compartments of the system (Peneva et al., 2001). The monthly runoff climatology for water fluxes was obtained from Kara et al. (2008) and are the same for all the six years. The surface salinity at the buffer zone was relaxed to a monthly climatology, computed from a 15-year simulation by the Copernicus Marine Environment Monitoring Service Black Sea circulation model (Storto et al., 2016). The salinity relaxation time is approximately two days. Although this is a strong constraint, it is required to prevent the surface salinity from decreasing in the buffer zone due to the excessive amount of fresh water input. The climatological values used for runoff and salinity relaxation are shown in Table 1.

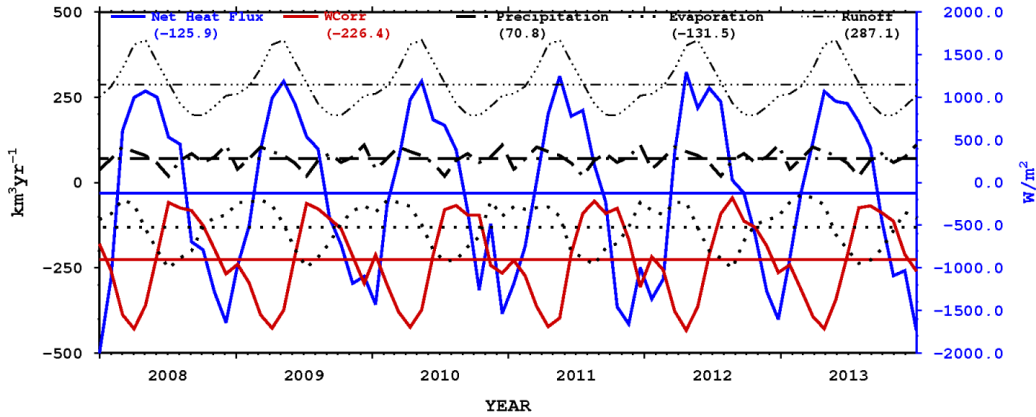
Here, we note again that the model having closed lateral boundaries requires a correction for the water and mass fluxes which we discuss in the Appendix A and B. Very briefly, the access or deficit of the water fluxes is redistributed to the surface model nodes weighted by the corresponding element area. Since a runoff climatology is inserted in the Black Sea to maintain the sea level difference along the system, the correction will enforce the volume conservation. This method was also used by Gent et al. (1998) for a climate global model. Another method was explored by Gürses et al. (2016) where the correction was applied only in the Aegean area but salinities became too high and the salinity profile of the simulation became unrealistic.

### 3 Results

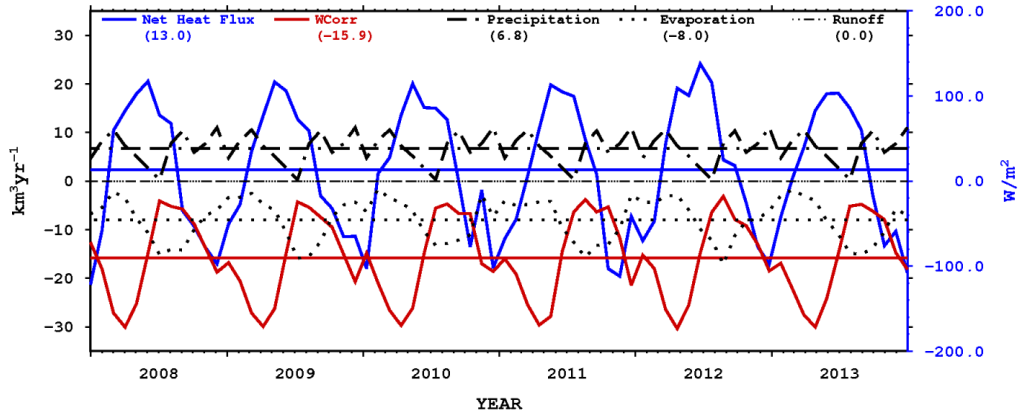
In this section, we present the results obtained from a simulation of the TSS between 2008 and 2013. The focus is on the Marmara Sea and the straits, but we also consider the adjacent basins when necessary. We provide details of the main water mass characteristics of the system and our validation against the observations. The sea level differences and the volume transports through the Bosphorus and Dardanelles are analysed. Although we will include results demonstrating the response of the system to daily atmospheric events, we focus on the interannual changes in the TSS. Therefore, we consider only annual means in time averages. The computed time averages for the simulation are for the period 2009-2013, as the first months of 2008 are considered as an initial spin-up period.

### 3.1 Surface Heat and Water Fluxes

The monthly averages of water fluxes and net heat flux in the Marmara Sea are shown in Fig. 3. The runoff is relatively small and is thus approximated to be zero in 3a for the whole domain and Fig. 3b for the Marmara Sea. The mean runoff, evaporation and precipitation in the whole domain are  $278.1 \text{ km}^3/\text{yr}$ ,  $-131.5 \text{ km}^3/\text{yr}$  and  $70.8 \text{ km}^3/\text{yr}$ , respectively. The resulting net water flux into the ocean is therefore  $226.4 \text{ km}^3/\text{yr}$  which is balanced by the correction term (see Appendix A) shown in red in Fig. 3a. As a result the model volume is conserved.



(a) Whole Domain



(b) Marmara Sea

**Figure 3.** Monthly averaged net heat (blue) and water (black) fluxes in the Marmara Sea, along with evaporation (dashed) and precipitation (dotted). Runoff is zero in the Marmara Sea. The blue vertical axis (right) is for heat flux and the black vertical axis (left) for water fluxes. Water flux correction described in appendix A is shown in red. Six-year mean values of fluxes are marked on the figures and shown in legends.

In the Marmara Sea, evaporation fluctuates between  $-5.1 \times 10^{-8}$  and  $-5 \times 10^{-9}$  m/s with an absolute minimum in March and a maximum in July. Minimum precipitation is  $1 \times 10^{-9}$  m/s in July while the maximum is  $3.3 \times 10^{-8}$  m/s in December. The resulting net water flux  $P - E$  varies between  $-4.7 \times 10^{-8}$  and  $2.5 \times 10^{-8}$  m/s, runoff is identically zero Fig. 3b. Mean evaporation and precipitation are  $8 \text{ km}^3/\text{yr}$  and  $6.8 \text{ km}^3/\text{yr}$ , respectively. The water flux correction applied in the Marmara Sea is  $-15.9 \text{ km}^3/\text{yr}$ . This means there is a net surface flux loss in the Marmara Sea about  $-17.1 \text{ km}^3/\text{yr}$ . The total water budget of the Marmara Sea will be further discussed in section 3.3.

The net heat flux in the Marmara Sea is calculated in the range of  $-123.3 \text{ W/m}^2$  to  $138.4 \text{ W/m}^2$  with minimums and maximums in December-January and May-June, respectively.

Monthly averaged net heat (grey) and water (black) fluxes in the Marmara Sea, along with evaporation (dashed) and precipitation (dotted). Runoff is zero in the Marmara Sea. The grey vertical axis (right) is for heat flux and the black vertical axis (left) for water fluxes.

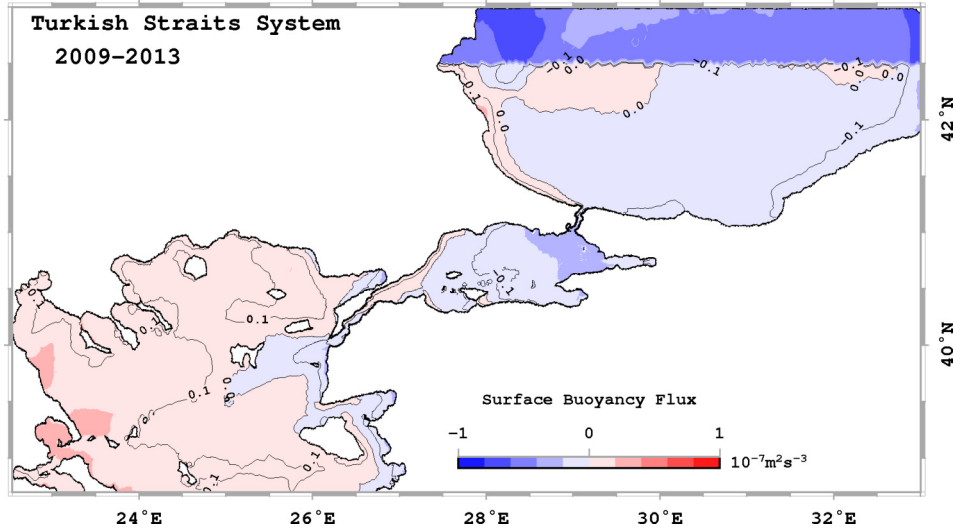


**Figure 4.** Mean of surface buoyancy fluxes for 2009-2013. A negative value is the buoyancy flux down into the ocean.

The daily buoyancy fluxes were averaged between 2009-2013 and are shown in Fig. 4. The buoyancy flux was computed using the formula:

$$Q_b = \frac{g\alpha}{\rho_0 C_w} Q_H - \beta S_0 g (E - P - R) Q_w \quad (2)$$

where  $\alpha$  and  $\beta$  are thermal and haline expansion coefficients (McDougall, 1987),  $Q_H$  is the heat flux (positive towards the ocean),  $C_w$  is the specific heat capacity,  $S_0$  is the surface salinity and  $E - P - R$  is the water flux.

The Black Sea and the Marmara Sea gain buoyancy except for a small area near their western coasts (Fig. 4), while the Aegean Sea has a buoyancy loss except near the Dardanelles exit and the Anatolian coast. The average buoyancy flux changes between  $-7 \times 10^{-8}$  and  $3.4 \times 10^{-8} \text{ m}^2 \text{ s}^{-3}$  over the domain. It does not show significant spatial differences interannually, but the gradient between the Aegean and Black Seas was stronger in 2011 than in the other years (not shown).

### 3.2 Water Mass Structure and Validation

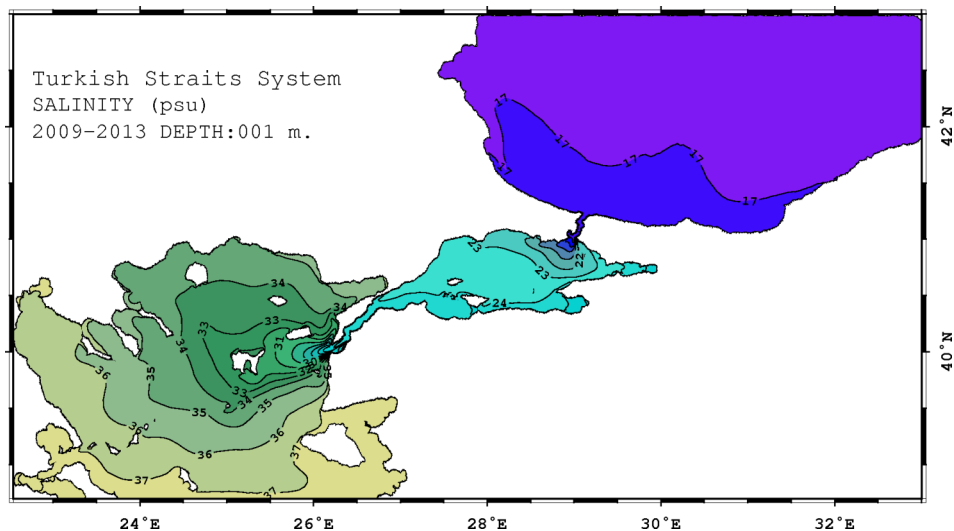


**Figure 5.** The mean sea surface salinity for 2009-2013. Contours are overlaid with 1 psu interval.

The surface salinity ranges from 16 to 38 psu over the whole domain (Fig. 5). The surface waters leave the Bosphorus and the Dardanelles with salinities of about 21 psu and 27 psu, respectively. The surface salinity in the northern Marmara Sea is less than 23 psu and increases to 25 psu in the south. Long-term measurements from 1986 to 1992 in the Marmara Sea (Beşiktepe et al., 1994) suggest a salinity ranging between  $23 \pm 2$  psu at the surface, which is satisfied by the simulation.

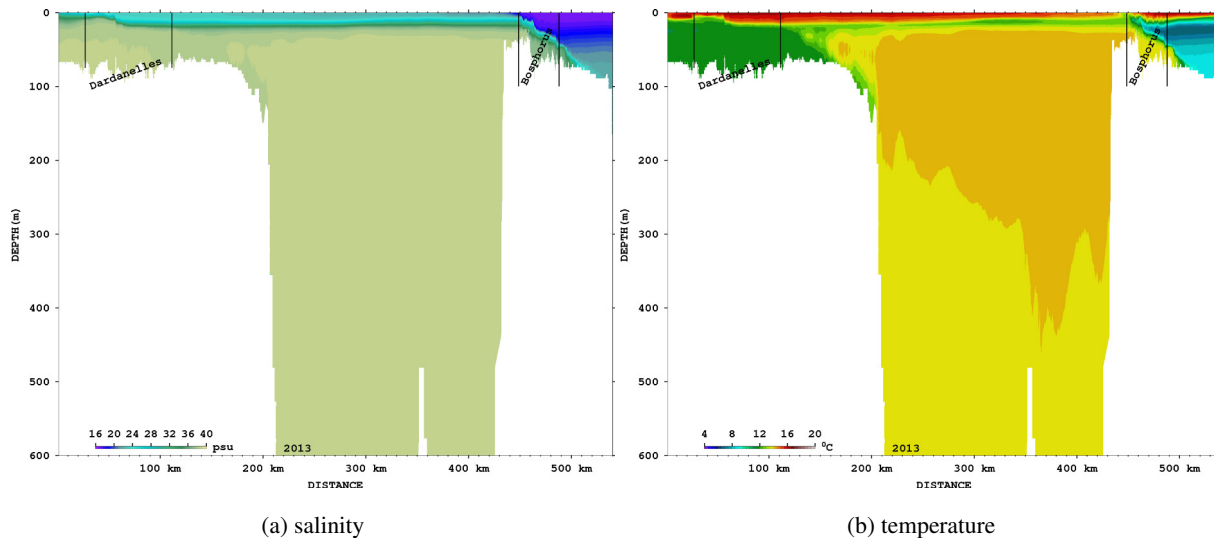


**Figure 6.** Annual mean of a) salinity and b) temperature for 2013 along the thalweg.

The vertical structure of the time mean salinity and temperature along the thalweg (see Fig.1) is shown for the last year of the integration in Fig. 6. The depth of the interface between the upper and lower layers is stationary throughout the simulation and is located at a depth of around 20 m. The water column salinity is mixed below 25 m in the Marmara Sea ~~whereas it is stratified in the straits.~~ until approximately 200 m. However, the deeper layers are colder and continuously modified by the Dardanelles inflow after the initialization as can be seen in Fig.7 in which the volume temperature has a negative trend and salinity a positive one. We argue that this is due to initialization adjustment and the closed boundary conditions. Salinity is completely mixed in the Marmara Sea below 100 m depth.

In the Bosphorus, Altıok et al. (2012) reported a cold tongue in the Bosphorus in June-July between 1996-2000, with a temperature of about 11-12°C, extending to the Marmara Sea. This cold tongue is reproduced in the simulation (Fig. 6b) and emerges as a cold intermediate layer (CIL) at the position of the halocline.

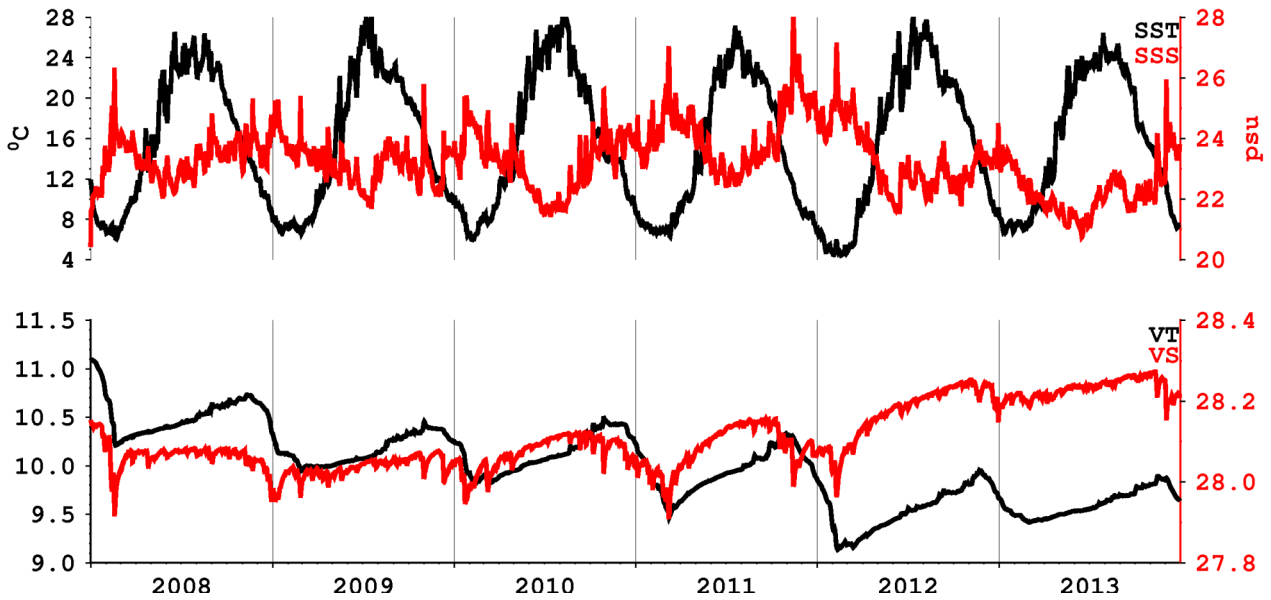


**Figure 7.** Daily time series of mean sea surface temperature (SST), mean sea surface salinity (SSS), volume mean temperature (VT), and volume mean salinity (VS) in the Marmara Sea. Temperature and salinity are shown in black and red, respectively.

The mean sea surface temperature in the Marmara Sea fluctuates between 4.4 - 28.3°C (Fig. 7). Surface mean salinities are lower in the spring and early summer than at other times of year. The volume mean temperature decreases from 11°C to 9-10°C and varies seasonally.

Three datasets of in-situ CTD observations were collected by R/V Bilim2 from the Institute of Marine Sciences (IMS/METU<sup>1</sup>), in 4-11 April 2008, 1-4 October 2008 and 18-23 June 2013 are used to validate the simulation.

	April 2008		October 2008		June 2013	
psu / °C	Salinity	Temperature	Salinity	Temperature	Salinity	Temperature
	1.34	0.77	1.71	1.09	3.18	2.09

**Table 2.** Mean RMS of salinity and temperature error with respect to CTD measurements in April and October 2008 and June 2013.

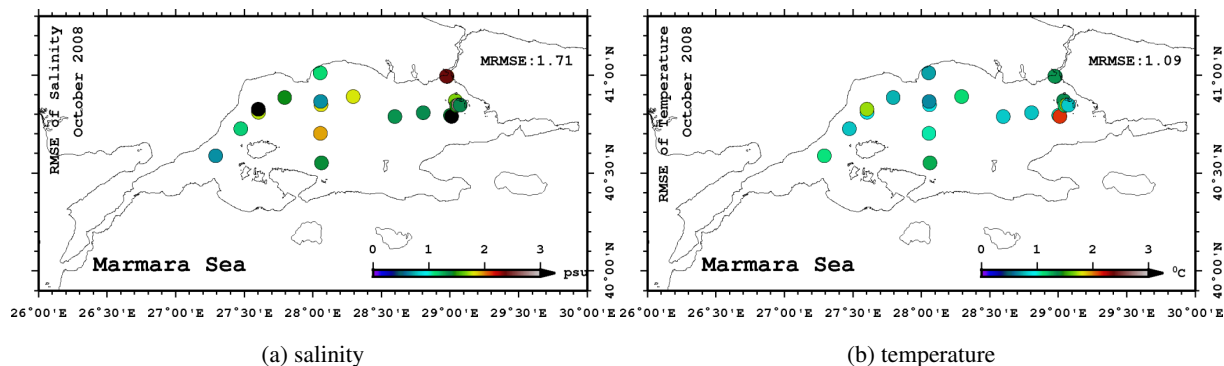


**Figure 8.** Spatial distribution of RMS of a) salinity and b) temperature error computed at the top 50 m of each CTD cast in October 2008

Figure 8 shows the spatial distribution of the salinity and temperature RMS errors in the first 50 m of the water column in October 2008. The error is higher in the eastern Marmara Sea close to the Bosphorus. The mean RMS errors of temperature and salinity are listed in Table 2. The errors are similar in April and October 2008, but notably increase after six years of integration in June 2013, which can be expected after such a long integration and, spatially, the errors are this time higher in the Dardanelles side of the Marmara Sea than the Bosphorus side. The RMS error is larger than those found in operational models of the Mediterranean Sea (Oddo et al., 2009), but this is due to a thermocline and halocline vertical shift, as shown in Fig. 9a. The vertical mixing and the missing interannual variability of the Black Sea runoff probably account for this. The model performs substantially better at the surface and below 30 m in depth than it does at the depth of the interface between the upper and lower layers of around 20 m (Fig. 9b). Temperature RMS errors are highest around the seasonal thermocline in June 2013, while at the same level as the halocline in the other two months.

<sup>1</sup> Two are from European SESAME-Southern European Seas: Assessing and Modeling Ecosystem Changes Integrated Project/ FP6. The other dataset is from the subsequent PERSEUS: Policy-oriented marine Environmental Research for the Southern European Seas, funded by the EU under the FP7 Theme 'Oceans of Tomorrow' OCEAN.2011-3 Grant Agreement No. 287600 project.

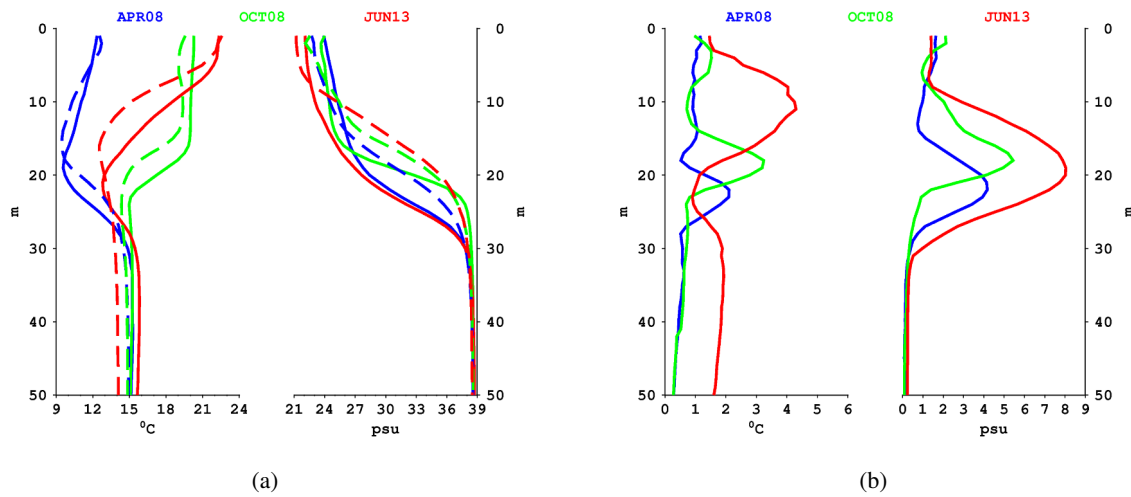


**Figure 9.** a) Mean temperature and salinity profiles of observations (dashed) and simulation (line) and b) vertical distributions of RMS errors in April 2008 (blue), October 2008 (green) and June 2013 (red).

### 3.3 Sea level and volume fluxes through the straits

The time mean of the sea surface height across the system is shown in Fig. 10 for the 2009-2013 period. The SSH is approximately 0.12 m in the Black Sea and -0.12 m in the Aegean Sea. In the Marmara Sea, SSH is higher in the western basin. The differences between the two ends of the Bosphorus are approximately 0.18 m and in the Dardanelles are about 0.11 m.

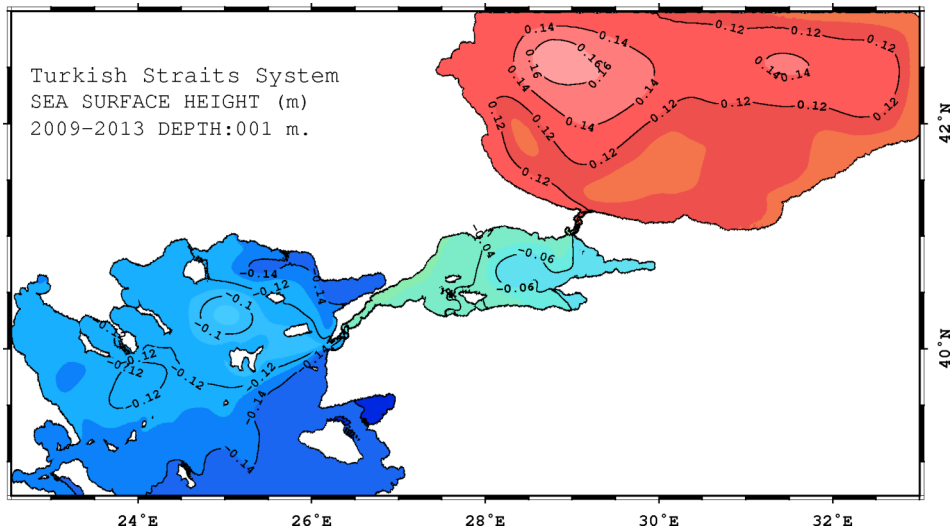


**Figure 10.** The mean sea surface height for 2009-2013. Contours are overlaid with 2 cm interval.

Moller (1928) measured the sea level differences between the two ends of the Dardanelles and the Bosphorus as 7 and 6 cm, respectively. Gunnerson and Ozturgut (1974) and Büyükay (1989) found the sea level difference in the Bosphorus to be 35 cm for the 1966-1967 period and 28-29 cm for 1985-1986 period, respectively. Bogdanova (1969) gave a sea level difference of 42 cm between the northern Black Sea (Ialta) and southern coast of Turkey (Antalya) with high seasonal variability. Alpar et al. (2000) suggested a mean sea level difference of 55 cm between the Black Sea entrance of the Bosphorus and the Aegean entrance of the Dardanelles for the 1993-1994 period. We cannot assess the accuracy of our model against these values in the literature with such a wide range of variability.

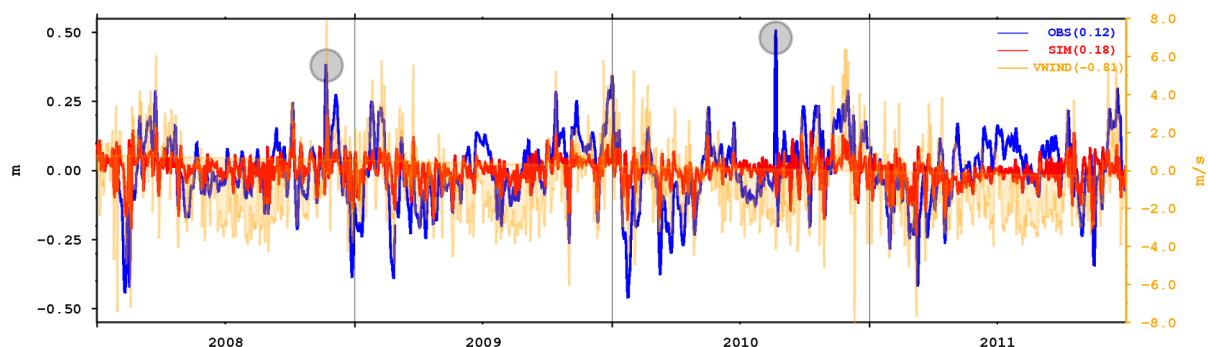
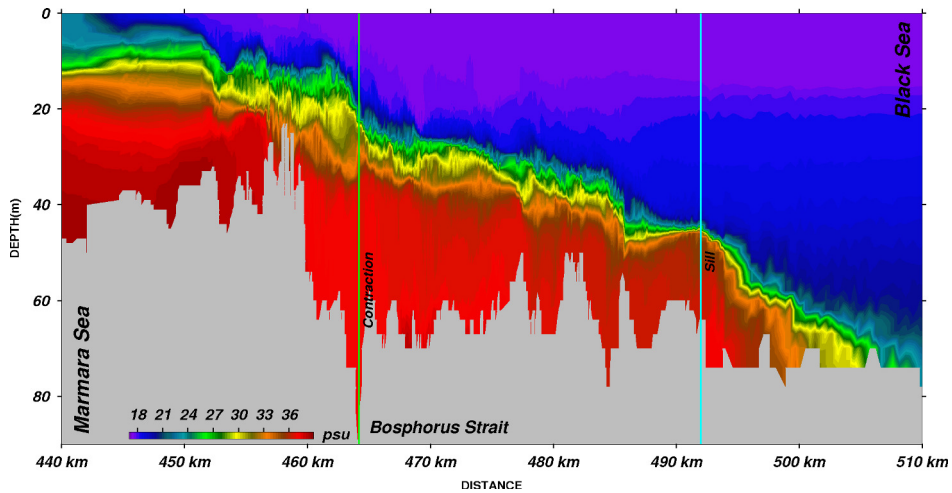


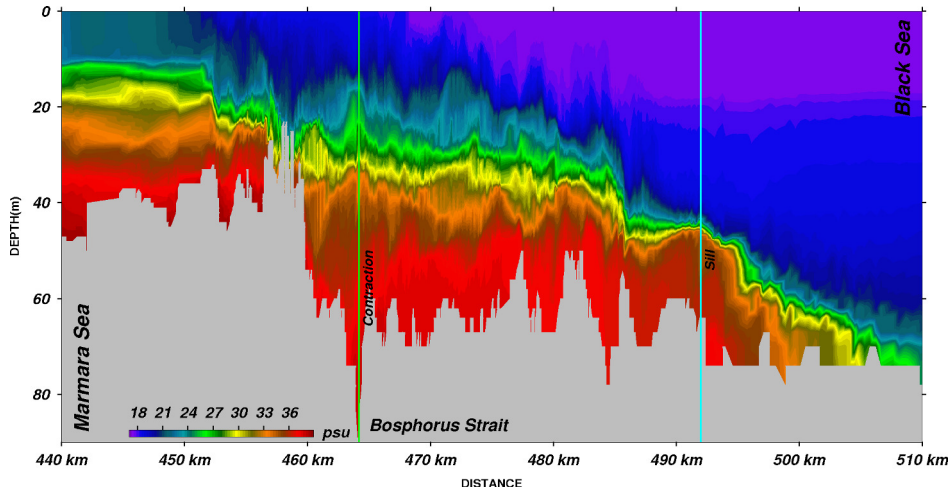
**Figure 11.** Sea level difference (SLD) between Yalova and Şile and daily averages of the meridional wind speed at B1 (See Fig. 1) between 2008-2011. The SLDs in the in-situ observation (OBS) and the simulation (SIM) in meters are shown by the blue and red lines, respectively. The meridional wind speed is in orange in meters per second. The four-year means, which are subtracted from the time series, are shown in the legend. A positive SLD means the sea level is higher in Yalova than in Şile. A positive wind speed means the wind direction is northward. The grey circles mark the Orkoz events in Nov. 22, 2008 and Aug. 21, 2010 as suggested by the observations.

As shown in Fig. 11, we compare the sea level difference between Yalova (Marmara Sea, see Fig. 1) and Şile (Black Sea) with the time series of tide gauge measurements collected between 2008 and 2011 (Tutsak et al., 2016). The [correlation between the observed and simulated sea level differences is 0.56](#). The response of the model is weaker during the arrival phase of severe storms, corresponding to southwesterly winds known as 'Lodos', when the sea level difference becomes negative in the observations; i.e., the sea level in the Marmara Sea is higher than in the southwestern Black Sea. The higher sea level in the Marmara Sea often results in short term blocking and reversal of the Bosphorus upper layer flow (called Orkoz). One such event was studied by Book et al. (2014) during the strong atmospheric cyclone passage of Nov 22, 2008 (Fig. 11). The signal of this event is captured in the sea level difference measurements (blue) and successfully reproduced by the model (red), though with a smaller amplitude. However, the event of 21 August 2010 is absent in the simulation as the atmospheric forcing (orange) shows no signal of a severe southerly storm. The accuracy of the atmospheric forcing is in this case limiting the correct oceanic response.

The salinity structure on Nov 15, 2008 represented in Fig. 12 along the thalweg line of Fig. 1 corresponds to the situation typically observed in the Bosphorus with a normal range of net flow. The features of the salinity distribution shown in Fig. 12a are similar to those shown by the measurements of Özsoy et al. (2001) and Gregg and Özsoy (2002), and computed by Sözer and Özsoy (2017a) and Sannino et al. (2017) respectively, in stand-alone Bosphorus and integrated TSS models of exchange



(a) Nov. 15 2008

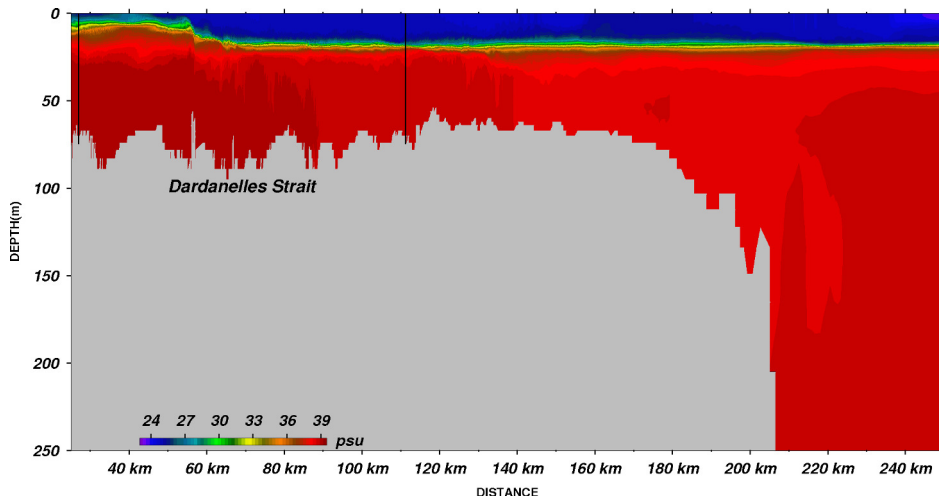


(b) Nov. 22 2008

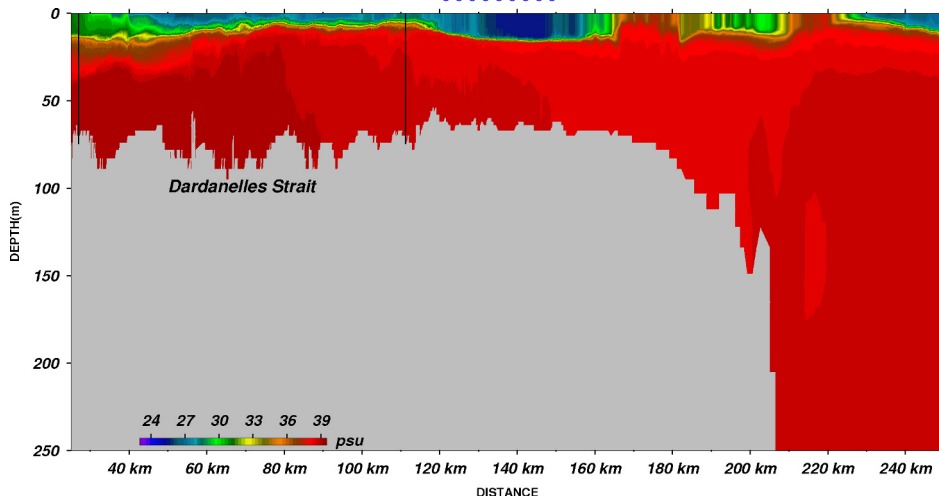
**Figure 12.** Cross-section of salinity in the Bosphorus Strait on a) Nov 15 b) Nov 22 2008 along the thalweg between 440-510 km. Contraction and the northern sill locations are marked with green and cyan lines, respectively, as shown in Fig. 1.

flows under a medium range of net flows excluding the effects of atmospheric forcing. The interface becomes thinner in the buoyant Bosphorus Jet flowing into the Marmara Sea and at the northern sill, where the lower layer reaches supercritical speeds through the hydraulic control, followed by a series of hydraulic jumps (Dorrell et al., 2016).

In comparison, the next section in Fig. 12b reflects the situation predicted in the Bosphorus on Nov 22, 2008. Under the conditions of an extreme Orkoz event, the upper layer flow of the Bosphorus becomes completely blocked. In rare instances the entire Bosphorus has been observed to flow towards the Black Sea, as reported after Nov 22, 2008, which was covered by a period of extensive measurements. ADCP measurements in the middle of the Bosphorus indicated a flow towards the Black



(a) [Nov. 15 2008](#)



(b) [Nov. 22 2008](#)

**Figure 13.** [Same as Fig. 12 but for the Dardanelles Strait and its Marmara Sea extension.](#)

Sea over the entire depth of the Strait, with superposed minor oscillations (Tutsak et al., 2016) during the event (Jarosz et al., 2011a; Book et al., 2014). The increased flow of dense water of mixed Mediterranean and TSS origin was found to cascade over the Black Sea shelf and propagate over large distances across the interior of the Sea at intermediate depths (Falina et al., 2017). The model results in Fig. 12 show increased vertical mixing in the upper layer up in the middle of the Bosphorus, but not all the way to the northern end as indicated by the measurements. The upper layer has been pushed north of the southern contraction, suggesting that the hydraulic control there has been lost. However, the thin interface layer on top of the northern sill and the flow north of it continues to preserve its shape, suggesting continued hydraulic control at the northern sill.

All the above features are consistent with the findings obtained from idealised and realistic models of the Bosphorus provided in Sözer and Özsoy (2017a) and the TSS model experiments of Sannino et al. (2017).

In the Dardanelles, the two-layered water mass and flow structure can be seen in Fig.13a. The simulated layered-structure in the Dardanelles is similar to those of (Sannino et al., 2017, Fig.7) under normal atmospheric conditions. The severe storm event in Nov. 22, 2008 results in extensive mixing in the upper layer (Fig.13b) where the salinity increases substantially. Furthermore, even the stratification is broken partially in the Marmara Sea side of the strait.

	UL $ u_{max} $ (m/s)	LL $ u_{max} $ (m/s)	Interface depth (m)
Northern Bosphorus	-0.35	1.4	40
Southern Bosphorus	-1.85	0.63	10
Northern Dardanelles	-1.0	0.78	20
Southern Dardanelles	-1.8	0.5	10

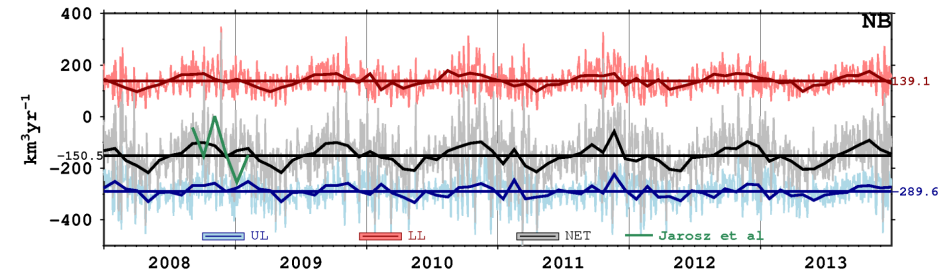
**Table 3.** Along-strait maximum velocity for the upper layer (UL) and lower layer (LL) and interface depth in each strait exit. Units are in  $m/s$  and  $m$  for the velocity and depth, respectively. A negative value means the flow in the direction from the Black Sea to the Aegean Sea.

Upper layer velocity in the southern exits of both the Bosphorus and Dardanelles are generally higher than their northern exits, due to the hydraulic controls exerted at the constrictions in the middle of both straits and the expansion area in the mouth (Sözer and Özsoy, 2017a). Conversely, the lower layer velocity has much higher maxima at the northern exits in both straits, and are roughly 0.2 m/s less than the measurements by Jarosz et al. (2011a, 2012). The upper layer maximum velocities are in accordance with most observations. The depth of the zero velocity level varies significantly in the exits of each strait and are listed in Table 3. These depths are consistent with the recent approximations reported in Jarosz et al. (2011a, 2012) for the northern Bosphorus, the southern Bosphorus, the northern Dardanelles and the southern Dardanelles, which are 39 m, 13.5 m, 22 m and 13 m, respectively.

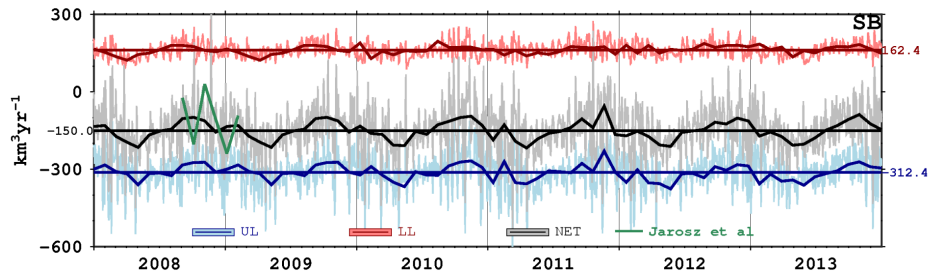
$km^3/yr$	Net	UL	LL
Northern Bosphorus	-147.7-150.5	-283.3-289.6	135.5-139.1
Southern Bosphorus	-148.5-150.0	-307.7-312.4	159.2-162.4
Northern Dardanelles	-104.2-132.8	-343.8-378.4	239.6-245.6
Southern Dardanelles	-102.3-130.7	-443.6-449.9	341.3-369.2

**Table 4.** Annual mean of net, upper layer and lower layer volume fluxes ( $km^3/yr$ ) for the whole simulation period. A negative value means the flux is in the Black Sea-Aegean Sea direction.

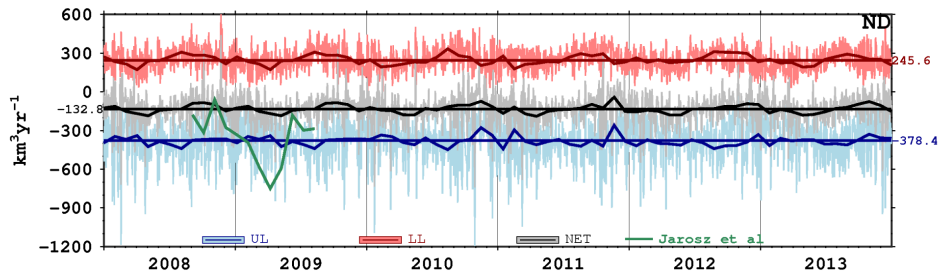
The net, annual mean upper layer and lower layer volume fluxes are given in Table 4 and the daily and monthly averages shown in Figure 14. The estimations from Jarosz et al. (2011b, 2013) from direct measurements are also indicated. The mean net volume fluxes through the straits compare well with the observations between 2 September 2008 and 5 February 2009 for the Bosphorus, and 1 September 2008 to 31 August 2009 for the southern Dardanelles. However, the variability in time is not



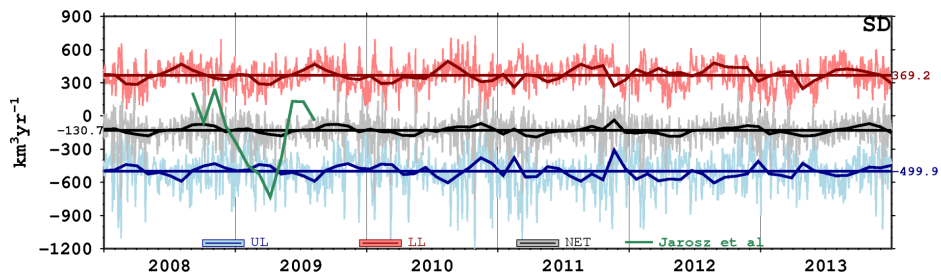
(a) Northern Bosphorus



(b) Southern Bosphorus



(c) Northern Dardanelles



(d) Southern Dardanelles

**Figure 14.** Daily upper layer (blue, UL), lower layer (red, LL) and net (grey, NET) volume fluxes through northern Bosphorus (NB), southern Bosphorus (SB), northern Dardanelles (ND) and southern Dardanelles (SD) in  $\text{km}^3\text{yr}^{-1}$ . Monthly and six-year averages are overlaid with a darker tone of the same colour. The monthly averages of volume fluxes computed by Jarosz et al. (2011b, 2013) are shown in green for the period of observations.

as high as in the observations (Figure 14). In the northern Dardanelles, there is a large discrepancy between the simulated net fluxes and the estimates from observations.

Sannino et al. (2017) and Özsoy and Altıok (2016) both have similar disagreements with the measurements of Jarosz et al. (2013) and have concluded that the discrepancies could be a result of measurement or computational inaccuracies at the wide northern section of the Dardanelles, where the instrument data were located.

The historical estimates of the Dardanelles layer volume fluxes show much higher values than our simulation (Table 5). The changes found in the layer flux from one end of the strait to the other have been attributed to turbulent entrainment processes, which transport water and properties across the hypothesised layer interface (Ünlüata et al., 1990; Özsoy et al., 2001; Özsoy and Altıok, 2016). The larger disagreement of baroclinic volume fluxes compared to the net fluxes, and the lower estimations of the model layer fluxes, suggest that bottom friction parametrization is too strong and possibly a problem in the vertical mixing submodel chosen.

Annual Fluxes ( $km^3/yr$ )	Northern Dardanelles			Southern Dardanelles		
	UL	LL	Net	UL	LL	Net
Ünlüata et al. (1990)	<del>-865.9</del> -866	566.0	<del>-299.9</del> -300	<del>-1257.0</del> -1257	<del>966.5</del> 957	<del>-290.5</del> -300
Beşiktepe et al. (1994)	-846.7	546.8	-299.9	-1217.6	917.7	-299.9
Özsoy and Ünlüata (1997)	-829.7	529.8	-299.9	-1179.7	879.8	-299.9
Tuğrul et al. (2002)	-918.6	597.9	-320.7	-1330.5	1009.7	-320.8
Kanarska and Maderich (2008)	-666.7	391.0	-275.7	-1224.2	946.0	-278.2

**Table 5.** Annual means of volume fluxes ( $km^3/yr$ ) through the Dardanelles estimated by different studies. UL, LL and Net stand for upper layer, lower layer and net fluxes, respectively. A negative value means the volume flux is from the Marmara Sea to the Aegean Sea.

The net volume transport in the model is approximately half of the historical estimations based on mass conservation laws assuming a net water flux into the Black Sea about  $300 km^3/yr$ . Our choice to conserve the model volume in a closed lateral boundary model by correcting the water flux every time step comes with the limitation of reducing the transport along its way from the Black Sea to the Aegean Sea. The total water flux over the Marmara Sea is  $-17.1 km^3/yr$  (Fig.3b) which is balanced by the difference between the southern Bosphorus and northern Dardanelles (Table 4). Due to the surface flux correction the net outflow in the Dardanelles is decreased by about 10% with respect what entered the Bosphorus. However, such correction allowed us to obtain realistic salinity profiles with respect to other correction methods such as Gürses et al. (2016).

Finally, the differences in transport between the transects at the two ends of each strait are  $0.5 km^3/yr$  and  $2.1 km^3/yr$  in the Bosphorus and Dardanelles, respectively. We attribute these differences partially again to the water flux correction at the surface. The rest is due to the numerical errors accumulating during the post-processing of the model outputs.

### 3.4 Marmara sea dynamics and circulation

Using the six-year simulation, it is now possible to estimate the kinetic energy input by the wind in the Marmara Sea.

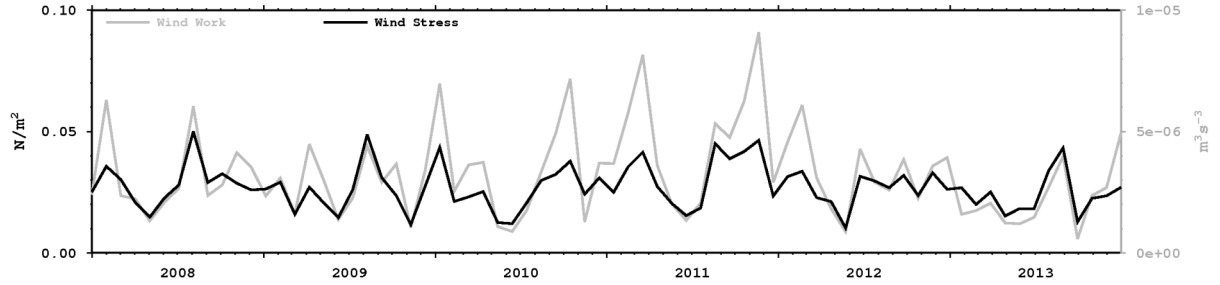


**Figure 15.** Monthly time series of the wind work ( $m^3s^{-3}$ ) and wind stress ( $Nm^{-2}$ ) in the Marmara Sea. The wind work normalised by the density and surface area of the Marmara Sea is shown in grey in the right vertical axis. The wind stress is the black curve and its values are shown on the left vertical axis.

The time series of monthly mean wind stress is shown in Fig. 15. It exhibits interannual differences with a mean of about  $0.03 Nm^{-2}$  and a maximum of around  $0.05 Nm^{-2}$  in August 2008. The monthly mean is highly variable and there is not a well-defined seasonal cycle between 2008-2013. The wind work normalised by the density and surface area is computed as:

$$\frac{1}{\rho_0 A} \int_A \tau \cdot \mathbf{u}_s dx dy \quad (3)$$

- 5 where  $\rho_0$  is the surface density,  $\tau$  is the wind stress,  $\mathbf{u}_s$  is the current velocity at the surface and  $A$  is the surface area of the Marmara Sea. The wind work is positively correlated with the wind stress. It is highest in 2011 and the maximum monthly mean wind work is  $9.1 \times 10^{-6} m^3s^{-3}$  in the autumn of 2011.

To compare with the other marginal seas described in Cessi et al. (2014), we normalise the right hand side of the equation 3 integral in (3) by the volume of the Marmara Sea instead of the surface area. The six-year mean of the wind work is computed as  $1.09 \times 10^{-8} m^2s^{-3}$ , one order of magnitude higher than the Mediterranean Sea. The wind work in the Baltic Sea was computed to be  $9.15 \times 10^{-9} m^2s^{-3}$ , which is comparable to the Marmara Sea but is still lower.

The resulting volume-mean kinetic energy in the Marmara Sea normalised by the unit mass is calculated as  $0.006 m^2s^{-2}$  for six years. The daily mean kinetic energy time series reveals that severe atmospheric events are able to energise the basin up to  $0.03 m^2s^{-2}$  (not shown). The monthly volume-mean kinetic energy averages fluctuate between  $0.005$ - $0.01 m^2s^{-2}$ . It is higher in winter and early spring, whereas it is always below the mean in summer. The highest kinetic energy inputs are in October 2010, April 2011 and November 2011. The kinetic energy is higher in the upper layer of the water column. The time-mean of surface kinetic energy is about  $0.03 m^2s^{-2}$ . Daily surface averages are capable of reaching  $0.2 m^2s^{-2}$ . The monthly mean increases to approximately  $0.05 m^2s^{-2}$  in November 2011.

In the Marmara Sea, the buoyancy gain is mainly due to the Bosphorus inflow, and thus the latter competes with the wind work to change the kinetic energy of the basin, as explained by Cessi et al. (2014). However, at the surface the kinetic energy shows that the Bosphorus surface jet energises the northeastern basin in addition to the wind (Fig. 16). The kinetic energy of the Bosphorus inflow is always greater than  $0.075 m^2s^{-2}$ . In 2009, a kinetic energy maximum appears in the north of the Bozburun peninsula where the Bosphorus jet arrives. In the western basin, the kinetic energy is generally less than  $0.025$

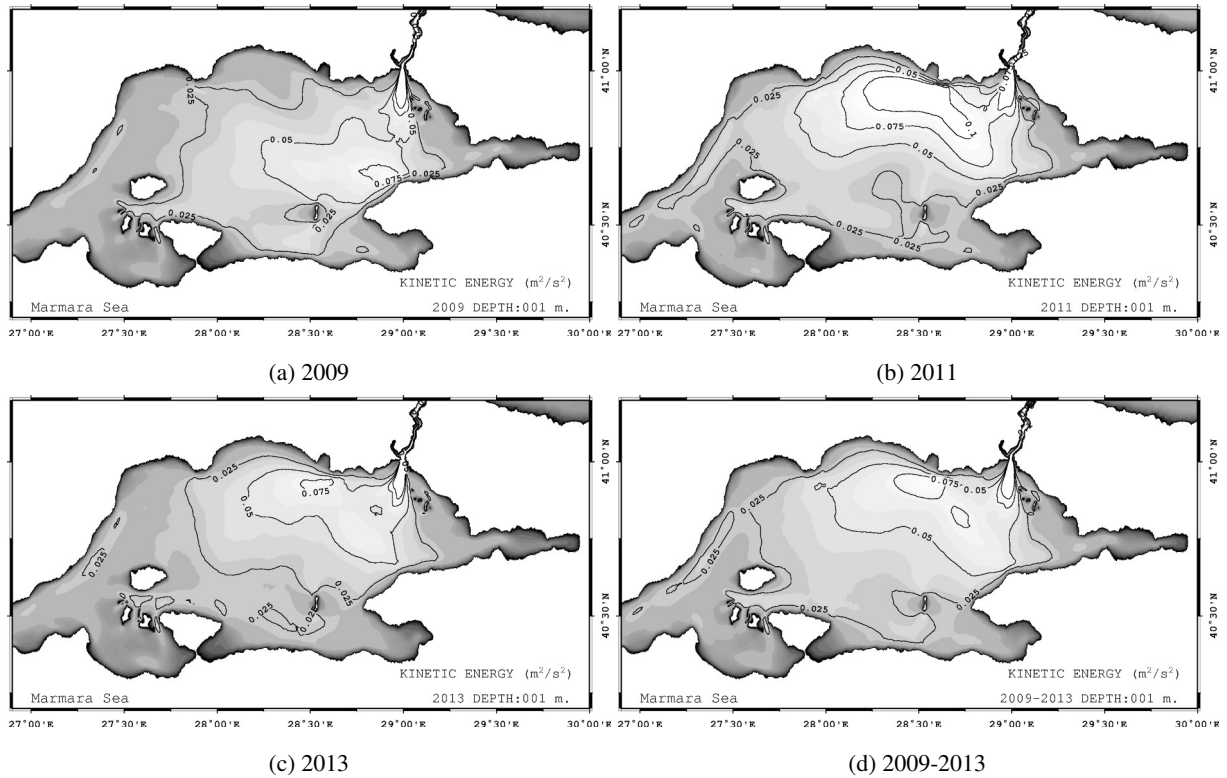


**Figure 16.** Annual mean of surface kinetic energy in the Marmara Sea for a) 2009 b) 2011 c) 2013. d) The time-mean of the 2009-2013 period. Units are in  $m^2s^{-2}$  as kinetic energy is normalised by the unit mass.

$m^2s^{-2}$ . In 2011, the kinetic energy intensifies in the central north and exceeds  $0.1 m^2s^{-2}$ . Almost all of the basin, except near the coastal areas, has a kinetic energy higher than  $0.025 m^2s^{-2}$ . Energy is mostly confined to the north-east of the central basin in 2013. The time-mean for 2009-2013 reflects the characteristics of 2011 but with less amplitude.

The energetic Bosphorus jet generates a dipole vorticity field, which is anti-cyclonic in the west and cyclonic in the east (Fig. 17). Northern and western coasts are dominated by anticyclonic vorticity. Conversely, cyclonic vorticity dominates the southern coast. Positive and negative vorticity in the northern and southern coasts of the islands and peninsulas, respectively, are other common structures for all the years. The mean vorticity fields are consistent with upwelling favourable conditions in the southern coasts of the Marmara Sea. Primarily, a cyclonic gyre located at  $28^{\circ}20',N - 40^{\circ}35',E$  forms in the central basin after 2011, showing that the circulation changed of sign sign between 2008 and 2011.

10 Fig. 18 shows the annual mean of the current velocity at the surface and 30 m for 2009, 2011 and 2013, and the mean for the 2009-2013 period. The annual means of the surface circulation show two different circulation structures as was already evident from the vorticity structures. In 2009 (Fig. 18a), the Bosphorus plume reaches the Bozburun peninsula and turns west towards the middle of the basin. One branch of the flow heads north and forms an anti-cyclone close to the Trachian coast. The southern branch instead splits into two when it reaches the Marmara Island. The southwestward flow traverses the Marmara

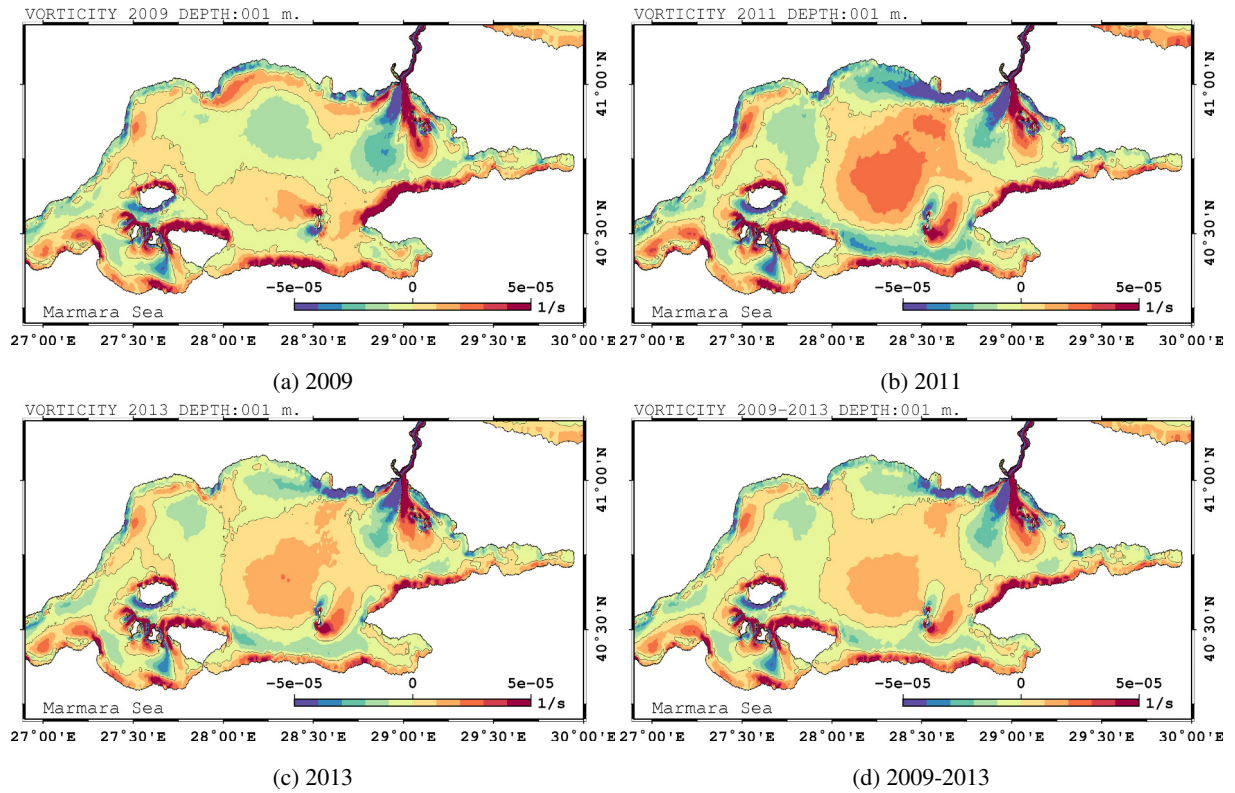


**Figure 17.** Annual mean of surface vorticity in the Marmara Sea at the surface. a) 2009 b) 2011 c) 2013, d) the surface vorticity mean for the 2009-2013 period.

Sea after turning south, merging with the flow circulating around the islands in the southwestern Marmara Sea and eventually exiting from the Dardanelles. This circulation pattern in the western Marmara Sea is persistent throughout the simulation but with different intensities. This type of circulation structure has been reported in other studies (Chiggiato et al., 2012; Beşiktepe et al., 1994). In 2011 (Fig. 18c), and the circulation in the middle of the Marmara Sea evolves into a single cyclonic structure.

5 The shift in the circulation can be explained by the shift of the wind stress maximum towards the north (Fig. 2). Sannino et al. (2017) demonstrates a similar cyclonic pattern in the central Marmara Sea due to the potential vorticity input by the Bosphorus. However, in our case, the main driver of the cyclone should be the wind as the volume transport through the Bosphorus is much lower than that of Sannino et al. (2017) case. Thus, in certain conditions both the wind and the Bosphorus can induce a cyclonic circulation in the Marmara Sea. The cyclonic surface circulation dominates the mean between 2009-2013. The mean surface

10 circulation in the Sea can be sketched as in Fig. 19.

Below the pycnocline at 30 m, two main structures can be identified. An anti-cyclonic formation appears in the central basin intensifying in 2013. On the Dardanelles side, a flow enters the Marmara Sea and partially heads south east. Another structure recirculates after reaching the Marmara Island and joins the southwestward flow exiting the Marmara Sea. In 2011, a meander

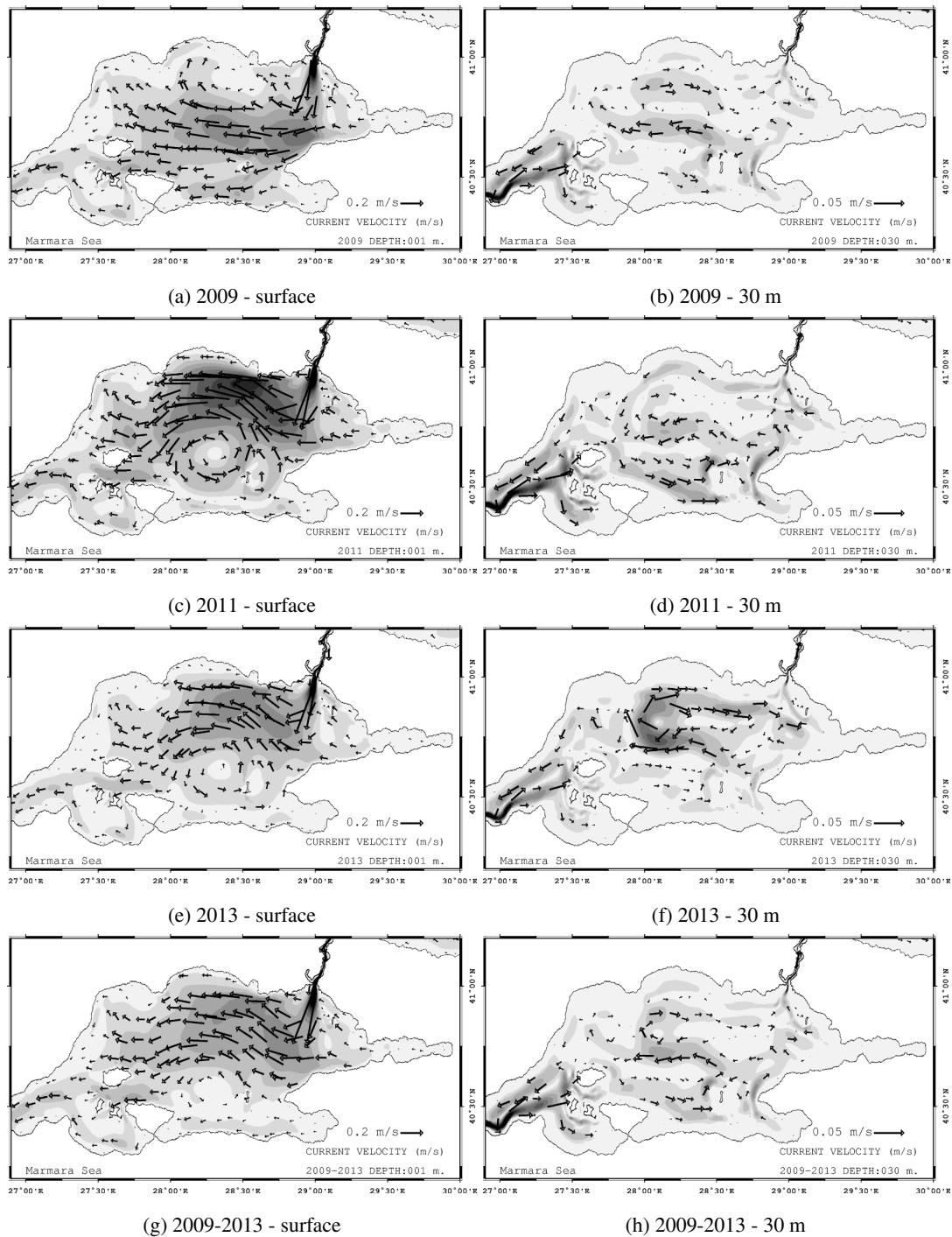


**Figure 18.** Annual mean of current velocity in the Marmara Sea. a) 2009 at the surface, b) 2009 at 30 m, c) 2011 at the surface, d) 2011 at 30 m, e) 2013 at the surface, f) 2013 at 30 m. The means for the 2009-2013 period are shown in g) at the surface and h) at 30 m

heading west is formed in the northern basin. This feature is not present in other years and results from the deepening of the upper layer (not shown) due to stronger wind stress.

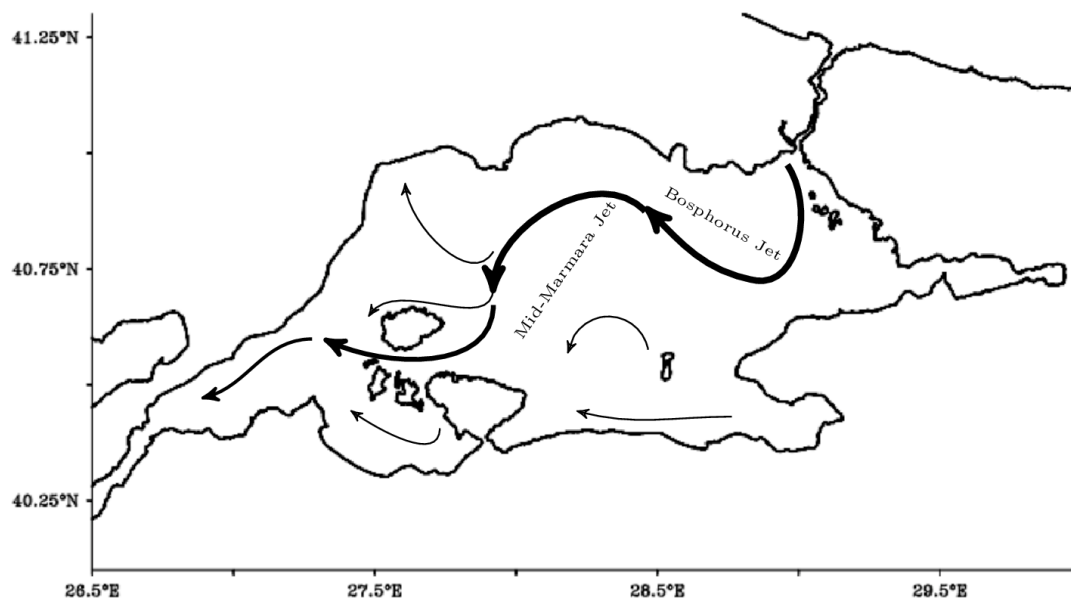


**Figure 19.** Schematic representation of the surface mean circulation in the Marmara Sea for the 2009-2013 period. The thickness of curves shows the relative intensity of the associated current.

The mean circulation of the Marmara Sea, schematically shown in Fig 19, is dominated by the Bosphorus jet and the mid-Marmara jet meandering cyclonically. The mid-Marmara jet is divided into three before reaching the Marmara Island, and one branch heads to the north west and other two reach the Dardanelles after circulating around the island. Finally, weak currents move in an east-west direction in the southern coast of the basin.

#### 4 Summary and discussion

We present a six-year simulation of the Turkish Straits System, with a highly resolved unstructured mesh model of the TSS using realistic atmospheric forcing to identify the circulation structure and the interplay between the atmospheric forcing and the Bosphorus input. The results demonstrate that a realistic representation of the pycnocline from the two Straits to the Marmara Sea is possible. The model is capable of reproducing the historically reported water mass structure of the Marmara Sea. Model errors peak at the halocline and thermocline depths, where small changes in the interface depth induce greater error.

The Strait volume transports have been compared with the observations. The net volume transports in the Bosphorus agree with the estimates based on the observations. The model solution departs from the observations in the northern Dardanelles, but closer agreement is found elsewhere. The baroclinic transports show larger discrepancies between the observations and the model, possibly because of uncertainties in the bottom boundary layer dissipation mechanisms and turbulence parameterization.

The model is capable of simulating blocking events in the straits during severe storm passages, to the extent that such storms are present in the atmospheric dataset, as shown for the 22 November 2008 case.

The circulation in the Marmara Sea shows two patterns in the interannual time scales. The first is dominated by the buoyant plume of the Bosphorus to the south around an anticyclonic circulation structure in the eastern and northern parts of the basin. This type of circulation has been observed and modelled by several earlier studies (Beşiktepe et al., 1994; Chiggiato et al., 2012; Sannino et al., 2017). The other circulation structure includes a cyclone in the central basin because of intensifying and expanding wind stress over the Marmara Sea. Small scale vortices are also formed in various parts of the basin and a larger one appears in the northwest after 2011. The cyclonic gyre in the central Marmara Sea is shown numerically only by Sannino et al. (2017), in the case of extreme net volume flux through the Bosphorus. However here we show that the wind can produce the cyclonic circulation in addition to the Bosphorus jet.

The long-term simulation with atmospheric forcing made it possible to evaluate the wind energy input and compute the kinetic energy in the Marmara Sea. The wind work in the Marmara Sea is shown to be even higher than the Baltic Sea. The high energy input from the wind significantly increases the kinetic energy in the Marmara Sea. During severe storms, kinetic energy can increase by 10 times the time-averaged value. The annual mean of kinetic energy in the regions under the influence of the wind forcing can also exceed that from the Bosphorus jet, depending on the wind stress structure.

In our modelling approach, we focused our attention on the TSS proper, which is the central domain including the Straits and the Marmara Sea, while assigning a limited storage role to the truncated exterior domains of the Black and Aegean Seas. This represents a trade-off between a truthful reproduction of the TSS circulation and the ability to impose far field boundary conditions in artificial closed basins at the two ends, using a similar strategy to that of Sannino et al. (2017). In future studies, we expect to obtain improved results by incorporating lateral open ocean boundary conditions in the Aegean and Black Seas. The skill of the model predictions also appeared sensitive to the accuracy of the atmospheric forcing used in the simulation. Within the relatively small domain of the TSS, an improved representation of the atmospheric forcing, particularly during the severe storms frequenting the region in winter, appears to be essential for improving its skill.

Overall, the results suggest further directions for long-term modelling in the TSS. We have demonstrated that wind forcing determines the surface circulation together with the Bosphorus inflow in the Marmara Sea. A higher resolution atmospheric forcing and better representation of the Black Sea water budget, by using open lateral boundaries, would improve the model solution particularly for the volume flux and the salinity flux estimations.

## Appendix A: Model Equations

FESOM solves the standard set of hydrostatic primitive equations with the Boussinesq approximation (Wang et al., 2008).

The momentum equations are:

$$\partial_t \mathbf{u} + \mathbf{v} \cdot \nabla_3 \mathbf{u} + f \hat{\mathbf{k}} \times \mathbf{u} = -\frac{1}{\rho_0} \nabla p - g \nabla \eta - \nabla A_h \nabla (\nabla^2 \mathbf{u}) + \partial_z A_v \partial_z \mathbf{u} \quad (\text{A1})$$

where  $\mathbf{u} = (u, v)$  and  $\mathbf{v} = (u, v, w)$  are 2D and 3D velocities, respectively in the spherical coordinate system,  $\rho_0$  is the mean density,  $p$  is the hydrostatic pressure obtained through integrating the hydrostatic relation (A3) from  $z=0$ ,  $g$  is the gravitational

acceleration,  $\eta$  is the sea surface elevation,  $f$  is the Coriolis parameter and  $\hat{k}$  is the vertical unit vector.  $\nabla$  and  $\nabla_3$  stand for 2D and 3D gradients or divergence operators, respectively. The horizontal and vertical viscosities are denoted by  $A_h$  and  $A_v$ . [p is the hydrostatic pressure obtained integrating the hydrostatic relation \(A3\) from  \$z = \eta\$ . Atmospheric pressure is not considered not to excite basin-modes in a closed lateral boundary model.](#)

- 5 The Laplacian viscosity is known to be generally too damping and strongly reduces the eddy variances of all fields compared to observations when the model is run at eddy resolving resolutions (Wang et al., 2008). Therefore, biharmonic viscosity is used in the momentum equations. Here,  $A_h$  is scaled by the cube of the element size with a reference value  $A_{h0}$  of  $2.7 \times 10^{13} m^4/s$  (Table A1), which is set for the reference resolution of 1 degree.

The continuity equation is used to diagnose the vertical velocity  $w$ :

$$10 \quad \partial_z w = -\nabla \cdot \mathbf{u} \quad (\text{A2})$$

and the hydrostatic equation is:

$$\partial_z p = -g\rho \quad (\text{A3})$$

where  $\rho$  is the deviation from the mean density  $\rho_0$ .

Tracer equations (A4) and (A5)

$$15 \quad \partial_t T + \mathbf{v} \cdot \nabla_3 T - \nabla \cdot K_h \nabla T - \partial_z K_v \partial_z T = 0 \quad (\text{A4})$$

$$\partial_t S + \mathbf{v} \cdot \nabla_3 S - \nabla \cdot K_h \nabla S - \partial_z K_v \partial_z S = 0 \quad (\text{A5})$$

- are solved for the potential temperature,  $T$ , and salinity,  $S$  where  $K_h$  and  $K_v$  are the horizontal and vertical eddy diffusivities, respectively. Laplacian diffusivity is used for the tracer equations.  $K_h$  is again scaled as  $A_h$  but by the element size with a reference value of  $2.0 \times 10^3 m^2/s$ . These values are set following the convergence study of Wallcraft et al. (2005).
- 20

The Pacanowski and Philander (1981) (PP) parametrization scheme is used for vertical mixing, with a background vertical viscosity of  $10^{-5} m^2/s$  for momentum and diffusivity of  $10^{-6} m^2/s$  for tracers. The maximum value is set to  $0.005 m^2/s$ .

The density anomaly  $\rho$  is computed by the full equation of state (A6).

$$\rho = \rho(T, S, p) \quad (\text{A6})$$

- 25 The surface and bottom momentum boundary conditions are, respectively:

$$A_v \partial_z \mathbf{u} = \tau \quad (\text{A7})$$

$$A_v \partial_z \mathbf{u} + A_h \nabla H \cdot \nabla \mathbf{u} = C_d \mathbf{u} | \mathbf{u} | \quad (\text{A8})$$

where  $\tau$  and  $C_d$  are the wind stress and the surface drag coefficient, respectively.

The surface kinematic boundary condition is:

$$w = \partial_t \eta + \mathbf{u} \cdot \nabla \eta + (E - P - R) + W_{corr} \quad (\text{A9})$$

where  $E$  (m/s),  $P$  (m/s) are evaporation and precipitation, respectively.  $R$  ( $km^3/yr$ ) is runoff ~~and~~ (see Table1). It is converted to  $m^3/s$  ~~before it is~~ and normalised by the area of the buffer zone in the Black Sea (see Fig. 1) ~~before entering to the equation~~. Finally,  $W_{corr}$  is a correction applied to conserve the volume of the model, as described later.

The sea surface height equation can now be derived from equations A2 and A9 as:

$$\partial_t \eta + \nabla \cdot \int_{z=-H}^{z=\eta} \mathbf{u} dz = -(E - P - R) - W_{corr} \quad (\text{A10})$$

The upper limit of integration in (A10) is set to  $\eta$  in this version of FESOM and is different from Wang et al. (2008) to provide a non-linear free surface solution.

The bottom boundary condition for the temperature and salinity are

$$(\nabla T, \partial_z T) \cdot \mathbf{n}_3 = 0 \quad (\text{A11})$$

$$(\nabla S, \partial_z S) \cdot \mathbf{n}_3 = 0 \quad (\text{A12})$$

where  $\mathbf{n}_3$  is the 3D unit vector normal to the respective surface.

The surface boundary condition for temperature is

$$K_v \partial_z T \Big|_{z=\eta} = \frac{Q}{\rho_0 C_p} \quad (\text{A13})$$

where  $C_p = 4000 J/(kg K)$  and  $Q$  ( $W/m^2$ ) is the surface net heat flux into the ocean.

In global applications, surface salinity is generally relaxed to a climatology to prevent a drift. In our regional application, the water flux term in the boundary condition (A14) is applied over the whole domain whereas the relaxation term is prescribed only in the Black Sea buffer zone.

$$K_v \partial_z S \Big|_{z=\eta} = S_0 (E - P - R) + \gamma (S^* - S_0) - S_{corr} \quad (\text{A14})$$

In the boundary condition (A14),  $S_0$  and  $S^*$  are the surface salinity and the reference salinity, respectively,  $\gamma$  is the relaxation coefficient (Table A1). Finally,  $S_{corr}$  is the counterpart of  $W_{corr}$  for salinity conservation corresponding to boundary conditions (A14), which will be defined in the following section.

PARAMETER	DESCRIPTION	VALUE	UNIT
$A_D$	Model Domain <u>Surface Area</u>	$1.52 \times 10^{11}$ <u>152 847</u>	$m^2 km^2$
$A_B$	Black Sea Buffer Zone Area	$2.26 \times 10^{10}$ <u>22 693</u>	$m^2 km^2$
$A_{MAR}$	<u>Marmara Sea Surface Area</u>	<u>10 707</u>	$km^2$
$A_{BOS}$	<u>Bosphorus Strait Surface Area</u>	<u>60.7</u>	$km^2$
$A_{DAR}$	<u>Dardanelles Strait Surface Area</u>	<u>301.3</u>	$km^2$
$R_B$	Black Sea Runoff	Table 1	
$S_0$	Sea Surface Salinity		psu
$S^*$	Salinity relaxed in the Black Sea Buffer Zone	Table 1	psu
$\gamma$	Salinity relaxation coefficient	$5.79 \times 10^{-6}$	$m/s$
$W_{corr}$	Water flux correction		$m/s$
$S_{corr}$	Salinity flux correction		$psu m/s$
$A_{h0}$	Horizontal eddy viscosity reference value	$2.7 \times 10^{13}$	$m^4/s$
$K_{h0}$	Horizontal eddy diffusivity reference value	$2.0 \times 10^3$	$m^2/s$
$A_{v0}$	Vertical background viscosity	$1.0 \times 10^{-5}$	$m^2/s$
$K_{v0}$	Vertical background diffusivity	$1.0 \times 10^{-6}$	$m^2/s$

**Table A1.** Parameters used in the model equations, surface boundary conditions and budget corrections.

## Appendix B: Salt Conservation Properties

As our model domain is closed we need to enforce salt conservation. Volume salinity conservation requires the time rate of the change in the volume salinity term in equation (B1) to be zero. A balance must be satisfied between the two integrals.

$$\frac{\partial}{\partial t} \iiint_V S dV = \iint_{A_D} (K_v \partial_z S|_{z=\eta}) dA_D = 0 \quad (\text{B1})$$

- 5 In FESOM, this balance is achieved by applying a correction for each term separately. The amount of water flux by evaporation, precipitation and runoff is integrated over the surface with every time step (Equation B2). After normalising by the domain area as in (B3), the surplus or deficit is added to or subtracted from the total water flux equally from each node of the mesh with the  $W_{corr}$  terms in equations (A9) and (A10).

$$\Delta_{(E-P-R)} = \int_{x,y} (E - P - R) dx dy \quad (\text{B2})$$

10

$$W_{corr} = \frac{\Delta_{E-P-R}}{A_D} \quad (\text{B3})$$

The salinity flux is corrected in a similar manner for the boundary condition

$$\Delta S = \int_{x,y} (S_0(E - P - R) + \gamma(S^* - S_0)) dx dy \quad (\text{B4})$$

$$S_{corr} = \frac{\Delta S}{A_D} \quad (\text{B5})$$

- 5 After applying these corrections, we get a surplus of water corresponding to about 1 mm of sea surface height increase a year, which we believe is due to random numerical errors. Correspondingly, the volume-mean salinity decreases by an order of  $10^{-5}$  psu a year. Although these errors may be significant in climate scales, they are acceptable for our six-year long experiment.

*Acknowledgements.* The simulation in this study are performed in CMCC/ATHENA cluster. The work is a part of the PhD study of Ali Aydođdu and funded by Ca Foscari University of Venice and CMCC. The preparation of this manuscript continued under the funding of  
10 the REDDA project of the Norwegian Research Council during his post-doctoral research. NCAR is sponsored by the US National Science Foundation.

## References

- Alpar, B., Doğan, E., Yüce, H., and Altıok, H.: Sea level changes along the Turkish coasts of the Black Sea, the Aegean Sea and the Eastern Mediterranean, *Mediterranean Marine Science*, 1, 141–156, 2000.
- Altıok, H., Sur, H. İ., and Yüce, H.: Variation of the cold intermediate water in the Black Sea exit of the Strait of Istanbul (Bosphorus) and its transfer through the strait, *Oceanologia*, 54, 233–254, 2012.
- Beşiktepe, Ş. T., Sur, H. İ., Özsoy, E., Latif, M. A., Oğuz, T., and Ünlüata, Ü.: The circulation and hydrography of the Marmara Sea, *Progress in Oceanography*, 34, 285–334, 1994.
- Bogdanova, C.: Seasonal fluctuations in the inflow and distribution of the Mediterranean waters in the Black Sea, In: *Basic Features of the Geological Structure, of the Hydrologic Regime and Biology of the Mediterranean Sea*, L.M. FOMIN, editor, Academy of Sciences, USSR, Moscow., 131–139, english translation 1969 Institute of Modern Languages, Washington DC, 1969.
- Book, J. W., Jarosz, E., Chiggiato, J., and Beşiktepe, Ş.: The oceanic response of the Turkish Straits System to an extreme drop in atmospheric pressure, *Journal of Geophysical Research: Oceans*, 119, 3629–3644, <https://doi.org/10.1002/2013JC009480>, 2014.
- Büyükkay, M.: The surface and internal oscillations in the Bosphorus, related to meteorological forces, Master's thesis, Institute of Marine Sciences, Middle East Technical University, Erdemli, İçel, Turkey, 1989.
- Cessi, P., Pinardi, N., and Lyubartsev, V.: Energetics of Semienclosed Basins with Two-Layer Flows at the Strait, *Journal of Physical Oceanography*, 44, 967–979, <https://doi.org/10.1175/JPO-D-13-0129.1>, 2014.
- Chiggiato, J., Jarosz, E., Book, J. W., Dykes, J., Torrisi, L., Poulain, P. M., Gerin, R., Horstmann, J., and Beşiktepe, Ş.: Dynamics of the circulation in the Sea of Marmara: Numerical modeling experiments and observations from the Turkish straits system experiment, *Ocean Dynamics*, 62, 139–159, <https://doi.org/10.1007/s10236-011-0485-5>, 2012.
- Courant, R., Friedrichs, K., and Lewy, H.: On the partial difference equations of mathematical physics, *IBM journal of Research and Development*, 11, 215–234, 1967.
- Danilov, S., Kivman, G., and Schröter, J.: A finite-element ocean model: principles and evaluation, *Ocean Modelling*, 6, 125–150, 2004.
- Demyshev, S., Dovgaya, S., and Ivanov, V.: Numerical modeling of the influence of exchange through the Bosphorus and Dardanelles Straits on the hydrophysical fields of the Marmara Sea, *Izvestiya, Atmospheric and Oceanic Physics*, 48, 418–426, 2012.
- Dorrell, R., Peakall, J., Sumner, E., Parsons, D., Darby, S., Wynn, R., Özsoy, E., and Tezcan, D.: Flow dynamics and mixing processes in hydraulic jump arrays: Implications for channel-lobe transition zones, *Marine Geology*, 381, 181–193, 2016.
- Falina, A., Sarafanov, A., Özsoy, E., and Utku Turunçoğlu, U.: Observed basin-wide propagation of Mediterranean water in the Black Sea, *Journal of Geophysical Research: Oceans*, 2017.
- Federico, I., Pinardi, N., Coppini, G., Oddo, P., Lecci, R., and Mossa, M.: Coastal ocean forecasting with an unstructured grid model in the southern Adriatic and northern Ionian seas, *Natural Hazards and Earth System Sciences*, 17, 45, 2017.
- Ferrarin, C., Bellafore, D., Sannino, G., Bajo, M., and Umgiesser, G.: Tidal dynamics in the inter-connected Mediterranean, Marmara, Black and Azov seas, *Progress in Oceanography*, 161, 102–115, 2018.
- Ford, R., Pain, C., Piggott, M., Goddard, A., De Oliveira, C., and Umpleby, A.: A nonhydrostatic finite-element model for three-dimensional stratified oceanic flows. Part I: model formulation, *Monthly Weather Review*, 132, 2816–2831, 2004.
- Gent, P. R., Bryan, F. O., Danabasoglu, G., Doney, S. C., Holland, W. R., Large, W. G., and McWilliams, J. C.: The NCAR climate system model global ocean component, *Journal of Climate*, 11, 1287–1306, 1998.

- Gregg, M. C. and Özsoy, E.: Flow, water mass changes, and hydraulics in the Bosphorus, *Journal of Geophysical Research: Oceans*, 107, 2002.
- Gunnerson, C. G. and Ozturgut, E.: The Bosphorus, The Black Sea—geology, chemistry and biology. *AAPG Bull*, 20, 99–114, 1974.
- Gürses, Ö., Aydoğdu, A., Pinardi, N., and Özsoy, E.: A finite element modeling study of the Turkish Straits System, in: *The Sea of Marmara - Marine Biodiversity, Fisheries, Conservations and Governance*, edited by Öztürk, B. et al., pp. 169 – 184, TUDAV Publication, 2016.
- Hüsrevoğlu, S.: *Modeling Of The Dardanelles Strait Lower-layer Flow Into The Marmara Sea.*, Master's thesis, Institute of Marine Sciences, METU, 1998.
- Ilicak, M., Özgökmen, T. M., Özsoy, E., and Fischer, P. F.: Non-hydrostatic modeling of exchange flows across complex geometries, *Ocean Modelling*, 29, 159–175, 2009.
- 10 Jarosz, E., Teague, W. J., Book, J. W., and Beşiktepe, Ş.: On flow variability in the Bosphorus Strait, *Journal of Geophysical Research: Oceans* (1978–2012), 116, 2011a.
- Jarosz, E., Teague, W. J., Book, J. W., and Beşiktepe, Ş.: Observed volume fluxes in the Bosphorus Strait, *Geophysical Research Letters*, 38, <https://doi.org/10.1029/2011GL049557>, 121608, 2011b.
- Jarosz, E., Teague, W. J., Book, J. W., and Beşiktepe, Ş.: Observations on the characteristics of the exchange flow in the Dardanelles Strait, 15 *Journal of Geophysical Research: Oceans*, 117, <https://doi.org/10.1029/2012JC008348>, c11012, 2012.
- Jarosz, E., Teague, W. J., Book, J. W., and Beşiktepe, Ş.: Observed volume fluxes and mixing in the Dardanelles Strait, *Journal of Geophysical Research: Oceans*, 118, 5007–5021, <https://doi.org/10.1002/jgrc.20396>, 2013.
- Johns, B. and Oğuz, T.: The modelling of the flow of water through the Bosphorus, *Dynamics of Atmospheres and Oceans*, 14, 229–258, 1989.
- 20 Jordá, G., Von Schuckmann, K., Josey, S., Caniaux, G., García-Lafuente, J., Sammartino, S., Özsoy, E., Polcher, J., Notarstefano, G., Poulain, P.-M., et al.: The Mediterranean Sea heat and mass budgets: estimates, uncertainties and perspectives, *Progress in Oceanography*, 156, 174–208, 2017.
- Kanarska, Y. and Maderich, V.: Modelling of seasonal exchange flows through the Dardanelles Strait, *Estuarine, Coastal and Shelf Science*, 79, 449–458, 2008.
- 25 Kara, A. B., Wallcraft, A. J., Hurlburt, H. E., and Stanev, E.: Air–sea fluxes and river discharges in the Black Sea with a focus on the Danube and Bosphorus, *Journal of Marine Systems*, 74, 74–95, 2008.
- Maderich, V. and Konstantinov, S.: Seasonal dynamics of the system sea-strait: Black Sea–Bosphorus case study, *Estuarine, Coastal and Shelf Science*, 55, 183–196, 2002.
- Maderich, V., Ilyin, Y., and Lemeshko, E.: Seasonal and interannual variability of the water exchange in the Turkish Straits System estimated 30 by modelling, *Mediterranean Marine Science*, 16, 444–459, 2015.
- Marshall, J., Adcroft, A., Hill, C., Perelman, L., and Heisey, C.: A finite-volume, incompressible Navier Stokes model for studies of the ocean on parallel computers, *Journal of Geophysical Research: Oceans*, 102, 5753–5766, <https://doi.org/10.1029/96JC02775>, 1997.
- McDougall, T. J.: Neutral surfaces, *Journal of Physical Oceanography*, 17, 1950–1964, 1987.
- Moller, L.: *Alfred Merz Hydrographische unter Suchungen in Bosphorus and Dardanalten*, Veroff. Insr. Meeresk, Berlin Uni., Neue Folge A, 35 18, 1928.
- Oddo, P., Adani, M., Pinardi, N., Fratianni, C., Tonani, M., and Pettenuzzo, D.: A nested Atlantic-Mediterranean Sea general circulation model for operational forecasting, *Ocean Science*, 5, 461–473, <https://doi.org/10.5194/os-5-461-2009>, 2009.
- Oğuz, T. and Sur, H.: A 2-layer model of water exchange through the Dardanelles strait, *Oceanologica Acta*, 12, 23–31, 1989.

- Oğuz, T., Özsoy, E., Latif, M. A., Sur, H. I., and Ünlüata, Ü.: Modeling of hydraulically controlled exchange flow in the Bosphorus Strait, *Journal of Physical Oceanography*, 20, 945–965, 1990.
- Özsoy, E. and Altıok, H.: A review of water fluxes across the Turkish Straits System, in: *The Sea of Marmara - Marine Biodiversity, Fisheries, Conservations and Governance*, edited by Öztürk, B. et al., pp. 42 – 61, TUDAV Publication, 2016.
- 5 Özsoy, E. and Ünlüata, Ü.: Oceanography of the Black Sea: A review of some recent results, *Earth-Science Reviews*, 42, 231 – 272, [https://doi.org/10.1016/S0012-8252\(97\)81859-4](https://doi.org/10.1016/S0012-8252(97)81859-4), 1997.
- Özsoy, E., Oğuz, T., Latif, M., Ünlüata, Ü., Sur, H., and Beşiktepe, Ş.: Oceanography of the Turkish Straits, Second annual report for the Istanbul Water and Sewerage Administration. Middle East Technical University, Institute of Marine Sciences, Erdemli, Turkey, 1988.
- Özsoy, E., Latif, M. A., Beşiktepe, S., Cetin, N., Gregg, M. C., Belokopytov, V., Goryachkin, Y., and Diaconu, V.: The Bosphorus Strait: Exchange fluxes, currents and sea-level changes, *NATO Science Series 2: Environmental Security*, 47, 1–28, 1998.
- 10 Özsoy, E., Di Iorio, D., Gregg, M. C., and Backhaus, J. O.: Mixing in the Bosphorus Strait and the Black Sea continental shelf: observations and a model of the dense water outflow, *Journal of Marine Systems*, 31, 99–135, 2001.
- Öztürk, M., Ayat, B., Aydoğan, B., and Yüksel, Y.: 3D Numerical Modeling of Stratified Flows: Case Study of the Bosphorus Strait, *Journal of Waterway, Port, Coastal, and Ocean Engineering*, 138, 406–419, [https://doi.org/10.1061/\(ASCE\)WW.1943-5460.0000132](https://doi.org/10.1061/(ASCE)WW.1943-5460.0000132), 2012.
- 15 Pacanowski, R. and Philander, S.: Parameterization of vertical mixing in numerical models of tropical oceans, *Journal of Physical Oceanography*, 11, 1443–1451, 1981.
- Peneva, E., Stanev, E., Belokopytov, V., and Le Traon, P.-Y.: Water transport in the Bosphorus Straits estimated from hydro-meteorological and altimeter data: seasonal to decadal variability, *Journal of Marine Systems*, 31, 21–33, 2001.
- Sannino, G., Sözer, A., and Özsoy, E.: A high-resolution modelling study of the Turkish Straits System, *Ocean Dynamics*, 67, 397–432, <https://doi.org/10.1007/s10236-017-1039-2>, 2017.
- Schroeder, K., Garcia-Lafuente, J., Josey, S., Artale, V., Buongiorno Nardelli, B., Carrillo, A., Gacic, M., Gasparini, G. P., Herrmann, M., Lionello, P., et al.: Circulation of the Mediterranean Sea and its variability, in: In: Lionello, P. (ed.), *The Climate of the Mediterranean Region—From the past to the future*, p. 592, Elsevier, 2012.
- Sözer, A. and Özsoy, E.: Modeling of the Bosphorus exchange flow dynamics, *Ocean Dynamics*, pp. 1–23, <https://doi.org/10.1007/s10236-016-1026-z>, 2017a.
- 25 Sözer, A. and Özsoy, E.: Water Exchange through Canal İstanbul and Bosphorus Strait, *Mediterranean Marine Science*, 18, 77–86, 2017b.
- Stanev, E. V., Grashorn, S., and Zhang, Y. J.: Cascading ocean basins: numerical simulations of the circulation and interbasin exchange in the Azov-Black-Marmara-Mediterranean Seas system, *Ocean Dynamics*, pp. 1–23, 2017.
- Stashchuk, N. and Hutter, K.: Modelling of water exchange through the Strait of the Dardanelles, *Continental Shelf Research*, 21, 1361–1382, 2001.
- 30 Storto, A., Ciliberti, S., Peneva, E., and Macchia, F.: Quality Information Document for Black Sea Physical Reanalysis product, Tech. rep., Copernicus Marine Environment Monitoring Service, 2016.
- Tutsak, E., Gündüz, M., and Özsoy, E.: Sea level and fixed ADCP measurements from the Turkish Straits System during 2008-2011, in: *The Sea of Marmara - Marine Biodiversity, Fisheries, Conservations and Governance*, edited by Öztürk, B. et al., TUDAV Publication, 2016.
- 35 Tuğrul, S., Beşiktepe, T., and Salihoglu, I.: Nutrient exchange fluxes between the Aegean and Black Seas through the Marmara Sea, *Mediterranean Marine Science*, 3, 33–42, 2002.
- Umgiesser, G.: SHYFEM finite element model for coastal seas, user manual, 2012.

- Ünlüata, Ü., Oğuz, T., Latif, M., and Özsoy, E.: On the physical oceanography of the Turkish Straits, in: *The physical oceanography of sea straits*, pp. 25–60, Springer, 1990.
- Wallcraft, A. J., Kara, A. B., and Hurlburt, H. E.: Convergence of Laplacian diffusion versus resolution of an ocean model, *Geophysical Research Letters*, 32, n/a–n/a, <https://doi.org/10.1029/2005GL022514>, 107604, 2005.
- 5 Wang, Q., Danilov, S., and Schröter, J.: Finite element ocean circulation model based on triangular prismatic elements, with application in studying the effect of topography representation, *Journal of Geophysical Research: Oceans (1978–2012)*, 113, 2008.
- White, L., Legat, V., and Deleersnijder, E.: Tracer conservation for three-dimensional, finite-element, free-surface, ocean modeling on moving prismatic meshes, *Monthly weather review*, 136, 420–442, 2008.
- Xie, P. and Arkin, P. A.: Global precipitation: A 17-year monthly analysis based on gauge observations, satellite estimates, and numerical  
10 model outputs, *Bulletin of the American Meteorological Society*, 78, 2539–2558, 1997.
- Zhang, Y. J., Stanev, E., and Grashorn, S.: Unstructured-grid model for the North Sea and Baltic Sea: validation against observations, *Ocean Modelling*, 97, 91–108, 2016.